Volume 4, October 2011

NDACC Newsletter

Network for the Detection of Atmospheric Composition Change

Exploring the interface between changing atmospheric composition and climate

The NDACC Newsletter is published by the NDACC Steering Committee. This is the fourth issue. The next issue is planned for the end of 2012.

Editor:

Geir O. Braathen

World Meteorological Organization

E-mail: GBraathen@wmo.int

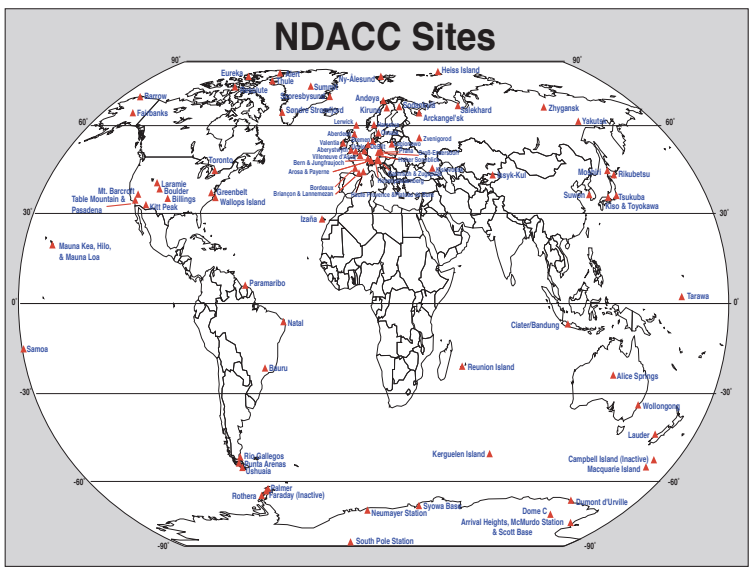

Cover photo: The German Antarctic station Neumayer. This is the third station at this site and it was inaugurated in February 2009. Photo: Alfred Wegener Institute for Polar and Marine Research (AWI).

Contents

Hot News

Termination of NDACC Primary and Complementary Station Designations

At the 2008 NDACC Steering Committee meeting, a decision was made to remove the "Primary" and "Complementary" designations of NDACC measurement sites / stations. These original terminologies were instituted at the inception of the Network for designating a minimum of five stations with long-term measurement commitments, representing the major geographical regions of the globe (i.e., Arctic, Northern Hemisphere (NH) Midlatitudes, Tropics, Southern Hemisphere (SH) Midlatitudes, and Antarctic). At that time, some of these stations were instituted as a combination of several sites, each with various types of instrumentation, such that the sum of all sites comprising a Primary Station included a fairly complete suite of NDACC (then NDSC) instrument types. It was anticipated that numerous Complementary Stations / Sites, at which a smaller number of Network-approved instruments were in operation, or at which the measurement commitment was for a shorter period of time, would augment these Primary Stations.

After nearly two decades of successful Network operations, the need for these designations no longer exists. In fact, their use now leads to some confusion and occasional misunderstanding. For example, some Complementary Sites have built up suites of instruments that are more comprehensive than those at some of the Primary Station sites. And many Complementary Stations / Sites have measurement commitments that are just as long-term as those at Primary Stations.

Further, these designations have occasionally been misinterpreted to imply that the measurements at and data from Complementary Stations are of lesser quality that those at Primary Stations, whereas the requirements to become affiliated with NDACC are identical for the two categories. There is no reduction in the expectations of instrument performance or data quality.

Lastly, some NDACC Principal Investigators felt that a Complementary designation was less advantageous than a Primary designation in justifying a long-term measurement need to their institution or funding agency.

From now on, all sites and stations will be designated simply as NDACC-approved measurement sites / stations. The NDACC Measurements and Analyses Directory is being revised to reflect this change, and measurement locations will be listed under one of the following groupings: NH High Latitudes, NH Midlatitudes, NH Subtropics and Tropics, SH Subtropics and Tropics, SH Midlatitudes, and SH High Latitudes.

Establishment of an NDACC Cooperating Network Affiliation

NDACC recognizes the importance of new measurement capabilities and of existing capabilities whose heritage was developed external to NDACC, and has encouraged Network affiliation with such measurements. In some cases, there are regional, hemispheric, or even global networks of instruments that operate independently of NDACC, but where strong measurement and scientific collaboration would be mutu-

ally beneficial. Such networks often have set up their own quality-assurance guidelines, operational requirements, and data archiving policies, and they have national or international recognition in their own right. In such cases, bringing the complete network under the NDACC umbrella is neither practical nor desirable. Rather, designation of an interested external network as a "Cooperating Network" may be more appropriate, and can foster collaborative measurement and analysis activities. For such designation to occur, the relevant NDACC Working Group must assess the benefits of mutual data access. The Working Group should further ascertain that the various protocols of the external network are compatible with those of NDACC, and are followed consistently and effectively. A protocol detailing the specific process whereby such affiliation can occur is posted on the NDACC web site. Agreements have been signed with these networks:

- AERONET/MPLNET
- AGAGE
- BSRN
- GEOmon
- NOAA HATS
- SHADOZ
- TCCON

Two New Measurement Capabilities Designated as NDACC-Approved

Since the onset of formal operations, NDACC (formerly NDSC) has designated several specific instrument types as official measurement capabilities. These are: Dobson / Brewer Spectrometers, Fourier Transform IR Spectrometers (FTIRs), Lidars (temperature, ozone, and aerosol), Microwave Radiometers, and UV/Visible Spectrometers. Balloon Sondes (ozone and aerosol) and UV Spectroradiometers were added shortly after the Network became operational. The Network strives to maintain the operation of as many of these instrument types within the various latitude regions as possible. As NDACC has matured, its measurement and analysis emphases have broadened to encompass issues such as the detection of trends in overall atmospheric composition and understanding their impacts on the stratosphere and troposphere, and establishing links between climate change and atmospheric composition. These challenges require an expansion of measurement capabilities, particularly in the area of some key climate parameters. Thus, after careful consideration and evaluation by the various NDACC Instrument Working Groups, the Steering Committee approved two new instrument types for NDACC designation: Raman Lidars for profile measurements of water vapour in the troposphere and across the tropopause, and Water Vapour Sondes (cryogenic frostpoint hygrometers and Lyman-a hygrometers) for profile measurements in the troposphere and stratosphere. Data from both instrument types soon will be available in the NDACC data archives.

New Species to Be Archived from FTIR Measurements

In the early days of NDACC (then NDSC), the Infrared Working Group (IRWG) targeted the retrieval of total columns of several gases considered of primary importance to the original goals of the Network. These goals focused on increasing our understanding of ozone chemistry and, in the post-Montreal Protocol

period, observing the accumulation (and hopefully the eventual decline) of Cl_y and F_y in the stratosphere. Consequently, the initial gases targeted were ozone, nitric acid (HNO_3), nitrous oxide (N_2O), chlorine nitrate ($ClONO_2$), hydrogen chloride (HCl), and hydrogen fluoride (HF). As the Network matured and science questions evolved to encompass the broader issues of climate change, attributing causal relationships for observed changes in atmospheric composition, and air quality, the IRWG reevaluated the ability of high-resolution mid-IR Fourier Transform Spectrometers to contribute and address the new scientific issues. At the 2008 IRWG meeting, the group agreed to add methane (CH_4), carbon monoxide (CO), hydrogen cyanide (HCN), and ethane (C_2H_6) to the existing suite of gases. All Principal Investigators in the IRWG maintain an archive of the recorded spectra since their observational program began, thereby allowing a re-analysis of these spectra. Consequently, the data record for the new gases will begin from the earliest observations for each site. Some of these data already are available to the public from the NDACC Data Host Facility. Many more will be archived during 2009.

Establishment of an Ad Hoc Working Group to Assess Future NDACC Measurement Strategies and Emphases

At the 2008 NDACC Steering Committee meeting, an ad hoc working group was established to review existing and assess future Network measurement strategies and emphases in light of the broadening of Network goals over those established at its inception. While NDACC remains committed to monitoring changes in the stratosphere with an emphasis on the long-term evolution of the ozone layer, its priorities now encompass issues such as the detection of trends in overall atmospheric composition, understanding their impacts on the stratosphere and troposphere, and establishing links between climate change and atmospheric composition. The members of this ad hoc working group (G. Braathen, M. Chipperfield, T. Deshler, S. Godin-Beekmann, J. Hannigan, K. Kreher, J.-C. Lambert, T. McElroy, R. McKenzie, G. Nedoluha, and W. Randel) solicit your input for their consideration. Email this group.

New web sites

IR WG

The Infrared Working Group has established a dedicated web site to describe their activities. It can be found here:

http://www.acd.ucar.edu/irwg/

Lidar WG

Also the Infrared Working Group has established a dedicated web site to describe their activities. It can be found here:

http://ndacc-lidar.org/

Also several other Working Groups have dedicated web sites. There are links to these in the left margin on the main NDACC web site: http://www.ndacc.org/

NDACC Welcomes NSF Spectral UV Instruments

NDACC welcomes new UV data from the United States National Science Foundation's network of UV spectrometers operated by Biospherical Instruments Inc. The spectral UV data set from this network is one of the longest and most extensive in existence, and covers geographical areas where ozone changes

have been most pronounced. Data summaries through November 2009 have been archived for most sites in the NDACC database. See http://UV.biospherical.com/ for other archivals. In our view it is crucial to maintain this network to monitor future changes in spectral UV irradiance. For further information, including examples of data products available, see the NDACC Spectral UV Working Group page.

Observational Capability Chart

The NDACC Observational Capability Chart shows the wide range of species and parameters that are measured with NDACC instruments. Bars with uniform colour represent column measurements and bars with ripples show measurements that are vertically resolved. The denser the ripples, the better the vertical resolution.

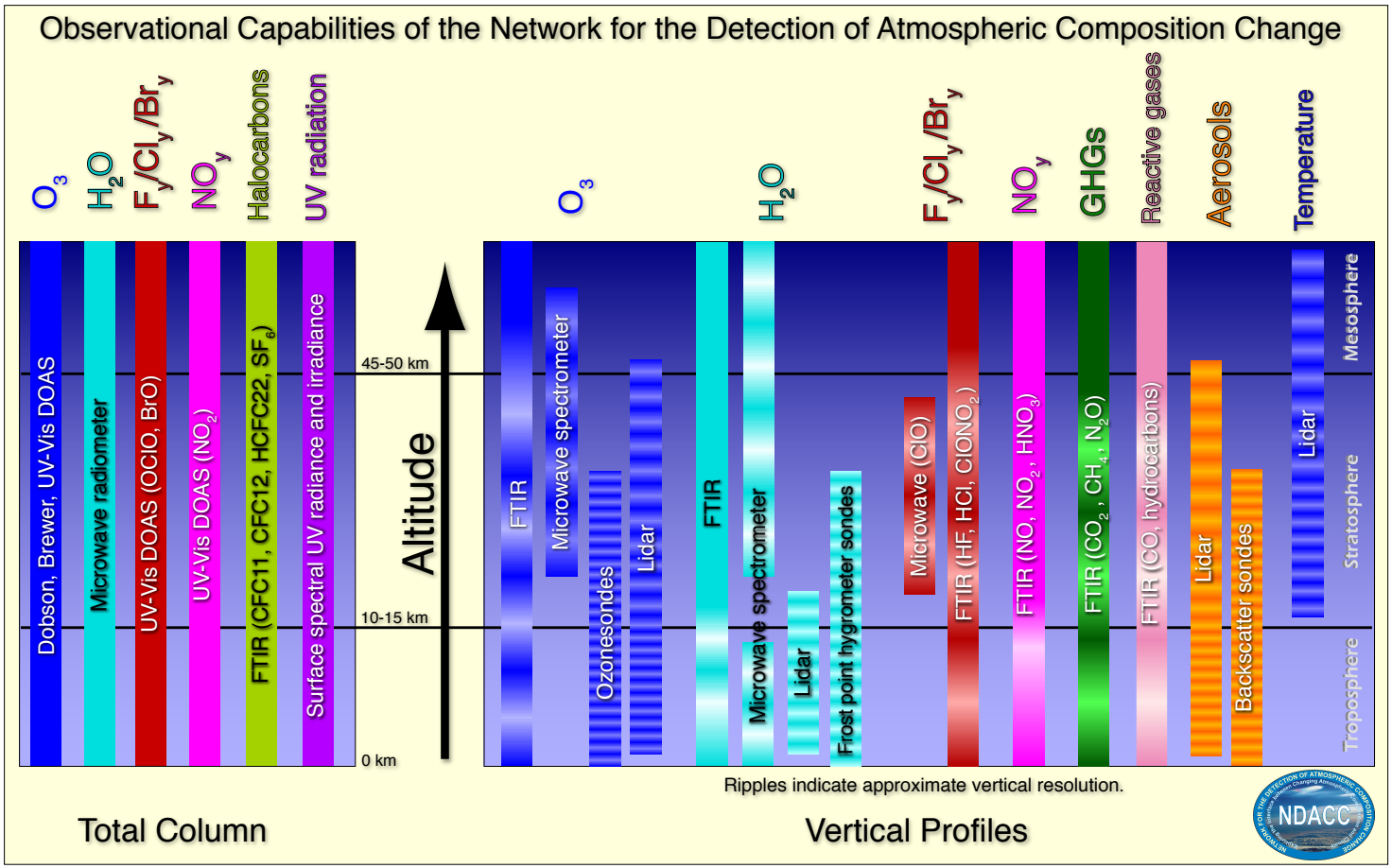

News from the Spectral UV Working Group

UV monitor at Palmer Station, Antarctic Peninsula. Photo: Germar Bernhard.

Long-Term UV measurements in Polar Regions

Germar Bernhard, Biospherical Instruments Inc., San Diego, California, USA and Richard McKenzie, National Institute of Water and Atmospheric Research (NIWA), Lauder, New Zealand

In 2009 NDACC welcomed data from the U.S. National Science Foundation's network of UV spectrometers operated by Biospherical Instruments. The data set from this netowrk is one of the longest in existence, and is from geographical areas where ozone changes have been most pronounced. In our view it is crucial to maintain this network to monitor future changes in UV.

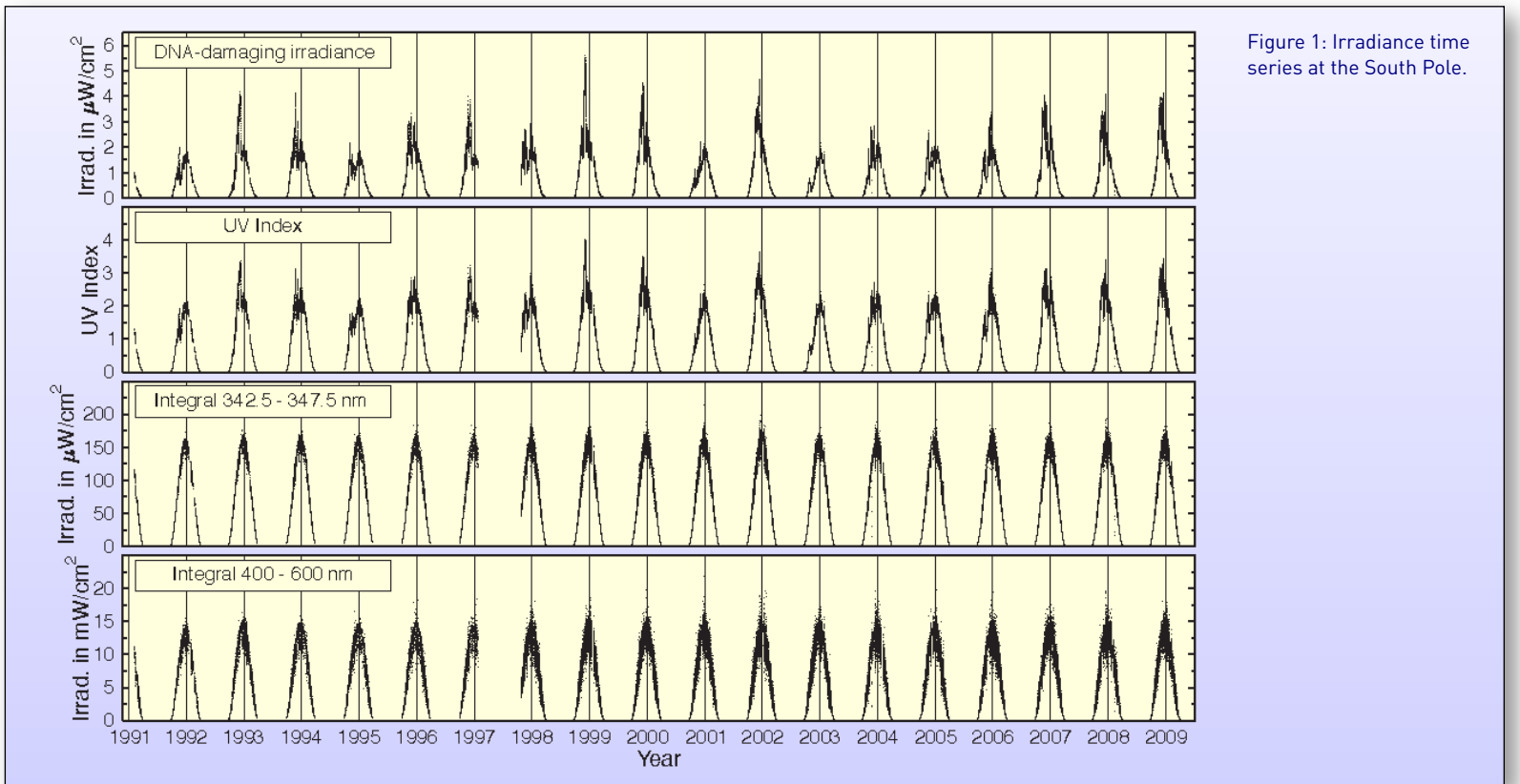

Figure 1: Irradiance time series at the South Pole.

Figure 1 shows time series of DNA-damaging irradiance, UV index, and integrals of 342.5–347.5 and 400– 600 nm at the South Pole. Data were measured by a SUV-100 spectro-radiometer that is part of the NSF UV Monitoring network, representing a subset of data submitted to the NDACC database. The graph includes measurements between October 1990 and March 2009 and is an extension of a similar dataset published by Bernhard et al. [2004].The figure indicates that DNA-damaging irradiance and the UV Index are very sensitive to changes in total ozone: for example, a one percent decrease in total ozone leads to approximately a 2.2% increase in DNA-damaging irradiance. Most of the day-to-day variability of these two data products is due the large variability in total ozone and the impact of the ‘‘ozone hole.” Largest radiation levels typically occur in late November and early December when low ozone columns coincide with relatively small SZA. Some years such as 1991, 1994, 2000, and 2003 appear to exhibit very little influence from the ozone hole, while other years such as 1992, 1993, 1996, 1998, 1999, 2001, 2006, 2007 and 2008 show a pronounced influence. This impression is somewhat deceptive as some years, such as 2000, displayed large relative enhance-ments in October when solar elevation and absolute values were still small.

Typical summer UV index values range between 2 and 3.5, with a maximum value of 4.0, measured on 11/30/98. Note that these values are significantly smaller than typical summer values for mid-latitudes. However, South Pole has 24 hours of daylight. Daily erythemal doses for the South Pole and San Diego, which were calculated by integrating erythemal irradi-ance over 24 hours, are therefore comparable.

The 342.5–347.5 nm integral is not affected by ozone and the influence by clouds is relatively small, partly because the contribution of the direct beam to global irradiance is less than 34% at all times, and partly because cloud attenuation is moderated by high albedo [Nichol et al., 2003]. As a con-sequence, the day-to-day and year-to-year variability is very small. The graph suggests that there is less variability for the years 1991–1997 than for years 1998–2009. Until January 1997, spectra were measured hourly, from February 1997 onward, one spectrum was measured every 15 min. The perception of larger scatter is not due to a real increase in variability but is apparent due to the four-times-higher sampling in the later years.

The 400–600 nm integral is more affected by cloud attenuation than the 342.5–347.5 nm integral, which explains the higher variability. Although ozone also absorbs weakly in the visible (Chappuis band), the contribution from changes in absorption in the Chappuis band to the overall variability is negligible.

Figure 2 compares measurements of spectral irradiance integrated over the range of 342.5–347.5 nm (right panel; hereinafter called “irradiance at 345 nm”) and the UV Index (right panel) as a function of SZA for the three sites, namely the South Pole; Summit, Greenland; and Barrow, Alaska.

The following can be concluded from the measurements at 345 nm:

- Measurements at Summit and South Pole are very similar.

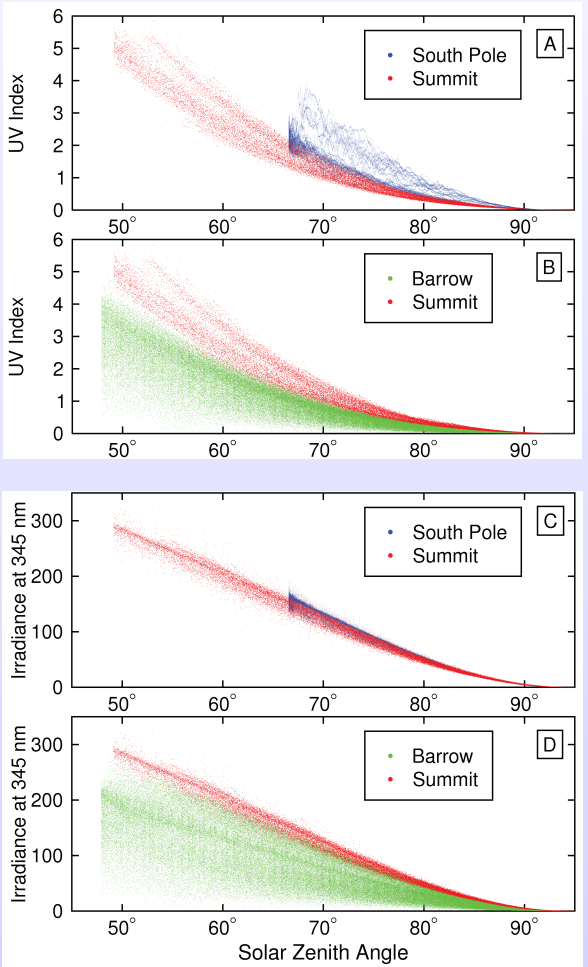

Figure 2: Comparison between sites and wavelengths of the SZA dependencies of measured irradiances. Upper panels (UV Index). Lower panels, UVA irradiance at 345 nm.

- The influence of clouds is very small at South Pole and Summit for two reasons: first, low temperatures over the ice caps lead to low atmospheric water content and optically thin clouds. Second, cloud attenuation is greatly moderated by high albedo due to multiple reflections between the snow-covered surface and clouds.
- Measurements at Barrow are substantially smaller than at Summit, mostly due to differences in cloudiness and surface albedo. The area of the highest point density in the Barrow data set is associated with clear-sky measurements during summer when albedo is low.

The following can be concluded from measurements of the UV Index:

- UV Indices are primarily controlled by the SZA.
- The overall maximum UV Indices are 6.7 at Summit, 5.0 at Barrow and 4.0 at South Pole.
- At SZA=70°, UV Indices vary between 0.8 and 1.8 at Summit, 0.0 and 1.2 at Barrow, and 1.0 and 3.4 at South Pole. Average, median, 5th, and 95th percentiles at SZA=70° are, respectively, 1.2, 1.2, 0.9, 1.6 for Summit; 0.7, 0.7, 0.3, 1.0 for Barrow; and 1.9, 1.7, 1.2, 2.9 for South Pole.
- For SZAs between 70° and 75°, UV Indices measured at South Pole during the period of the ozone hole exceed maximum indices observed at Summit by 50–60% on average.
- For times not affected by the ozone hole, measurements at South Pole are comparable to maximum indices at Summit, but the majority of measurements at Summit are considerably below South Pole levels.
- UV Indices at Summit exceed UV Indices at Barrow by more than 50% on average.

Figure 3 compares the maximum daily UV Index ever measured at Palmer Station, Antarctica, San Diego, and Barrow, Alaska. The maximum daily UV Index is a measure of peak sunburning UV that occurs during the day at a particular location. For Palmer Station, the figure also shows an estimate of the annual cycle of the UV index for the time period of 1978-1980, i.e. before development of the ozone hole. This data set is based on model calculations taking into account satellite ozone measurements and assumption on the annual cycles of surface albedo and attenuation by clouds. The figure shows that the UV Index is higher in San Diego than in Barrow throughout the year. Index values are zero at high latitudes when darkness is continuous. The effect of ozone depletion on the Index is demonstrated by comparing the Palmer and San Diego data. Normal values estimated for Palmer are shown for the 1978-1980 period before the "ozone hole" occurred each season (thin red line). In the last two decades (1990-2006), Antarctic ozone depletion has led to an increase in the maximum UV Index value at Palmer throughout spring (see yellow shaded region). Values at Palmer are now sometimes equal to or even exceeding those measured in spring in San Diego, which is located at a much lower latitude.

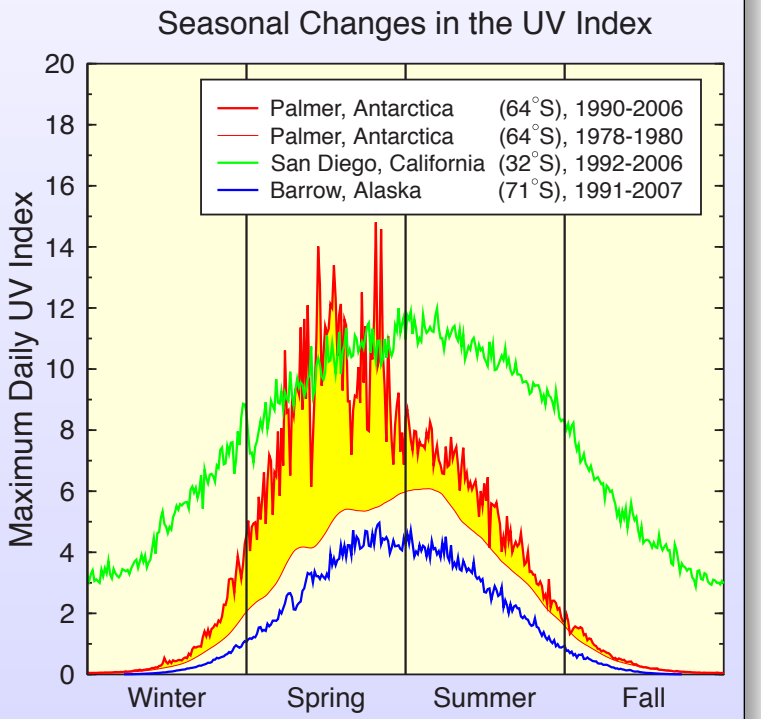

Figure 3: Changes in UV Index. The maximum daily UV Index is a measure of peak sunburning UV that occurs during the day at a particular location. UV-B, which is absorbed by ozone, is an important component of sunburning UV. The UV Index varies with latitude and season as the Sun's path through the local sky changes. The highest values of the maximum daily UV Index occur in the tropics where the midday Sun is highest throughout the year and where total ozone values are lowest. For comparison, the figure shows that the UV Index is higher in San Diego than in Barrow throughout the year. Index values are zero at high latitudes when darkness is continuous. The effect of ozone depletion on the Index is demonstrated by comparing the Palmer and San Diego data in the figure. Normal values estimated for Palmer are shown for the 1978-1983 period before the "ozone hole" occurred each season (see red dotted line). In the last decade (1991-2001), Antarctic ozone depletion has led to an increase in the maximum UV Index value at Palmer throughout spring (see yellow shaded region). Values at Palmer now sometimes equal or exceed those measured in spring in San Diego, which is located at a much lower latitude. From FAQ 17-2 in the WMO/UNEP Scientific Assessment of Ozone Depletion: 2006.

News from the Dobson and Brewer Working Group

Intercomparison of Dobson spectrophotometers at Hohenpeissenberg, Germany in 2007. Photo: Ulf Köhler.

Ten years of RDCC-E at the Meteorological Observatory Hohenpeissenberg

Ulf Köhler, Meteorological Observatory Hohenpeissenberg, Deutscher Wetterdienst (DWD), Germany

The general structure of the QA/QC (Quality Assessment/ Quality Control) in the Dobson network has already been described in the 2008 NDACC Newsletter. As a part of this structure the Regional Dobson Calibration Center for the WMO RA VI Europe (RDCC-E) at the Meteorological Observatory Hohenpeissenberg (MOHp) in close co-operation with the Solar and Ozone Observatory Hradec Králové (SOO-HK) has been in operation now for 10 years. Officially dedicated in 1999 the first regular International Dobson intercomparisons were organized in 2000. In the meanwhile a large number of various activities like regular Dobson calibrations, upgrades to the new electronic, relocations of Dobsons and calibrations of the regional standards towards the world standard Dobsons have been performed.

In the following a summary of these activities and the positive effects for the QA/QC-programme will prove the benefit for the global ozone monitoring network.

The main task of such an RDCC is to calibrate the Dobsons in its region every four to five years according the WMO recommendations. During such calibration campaigns the Dobsons are normally undergone a so-called initial calibration, which defines the status of the instrument. A difference to the reference instrument with only a small mu-dependancy (mu is the relative optical pathlength through the ozone layer) of less than ±1 % indicates, that the Dobson has been stable since the last intercomparison and does not need any optical work. There are, however, sometimes instruments, which obviously have optical deficits, which cannot be eliminated only by application of new calibration constants. The Dobson No. 35 is an outstanding example, as it was dropped at the London Airport during transportation from Boulder back to London in 1998 after a calibration there. Tests and observations at the station showed, that there must be something wrong with the optical alignment. The following calibration service at the RDCC-E proved this suspicion and the following optical alignment could solve the problem significantly (Figure 1).

Calibration of Dobsons from UK, Antarctica (British Antarctic Survey) and Greenland in 2004. Photo: Ulf Köhler.

Fortunately only a small number of instruments needs such an intense treatment to improve function. Up to now 76 Dobsons from 27 countries have been undergone a calibration service at the RDCC-E. Eighteen campaigns were organized at MOHp, eight at other facilities like Arosa, El Arenosillo, Hradec Králové). In addition, the crew of MOHp gave support to five campaigns, two of them organized by the RDCC for Africa (South African Weather Service). This support can be seen as capacity building and is partly financed by an ESA funded project.

Before this calibration task can be fulfilled, the existence of a well-calibrated, stable regional reference Dobson must be guaranteed. The selected European standards D064 (MOHp) and D074 (SOO-HK) had been proved as very stable instruments ten years ago. Eight (D064) and five (D074) calibrations towards the world standards from NOAA (Boulder) D083 and D065 since 1999 have confirmed that both instruments can be used as transfer instruments for the primary calibration level into the European network (Figure 2).

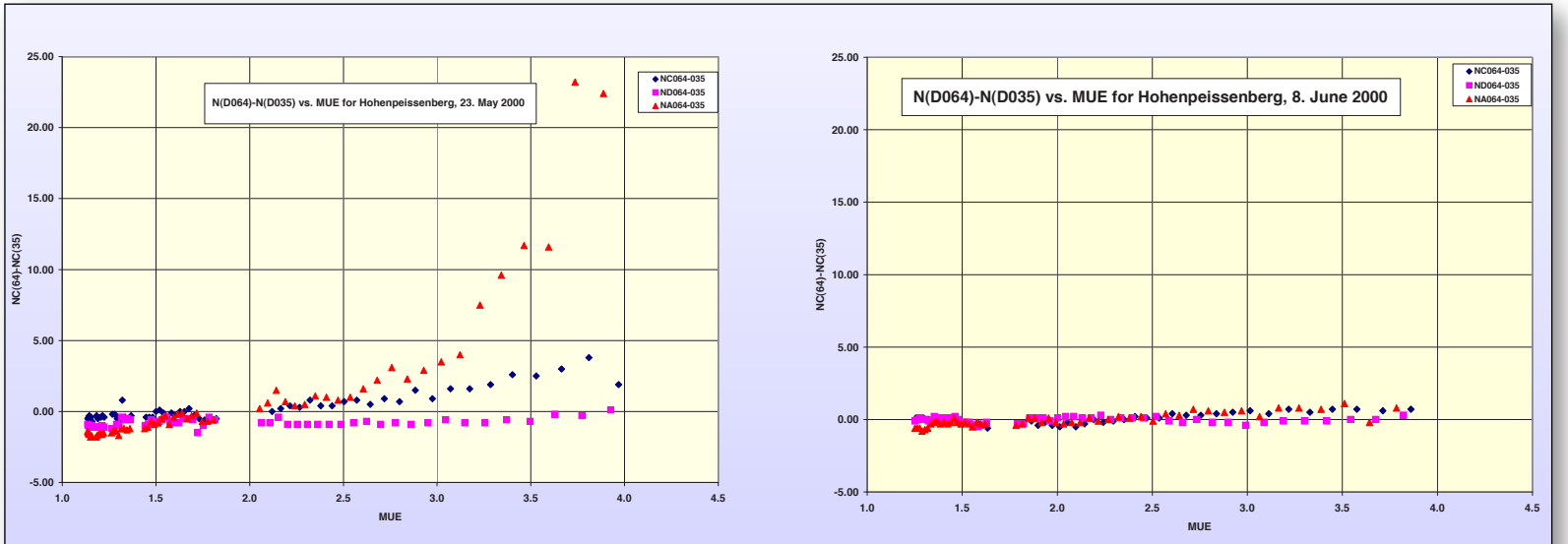

Figure 1: The original data (23 May 2000) show big discrepancies to the reference instrument, especially in the A wavelength pair. This could be significantly improved after optical re-alignment (adjusted data, 8 June 2000).

Whereas most of these calibrations were conducted as regular intercomparisons, the campaigns at the Izaña Observatory on Tenerife in 2008 (D064, D074, D083) and 2010 (D064) were performed as special Langley observations, to provide absolute calibrations for the standard Dobsons and to compare the results. Table 1 shows that the derived corrections to the existing calibration levels resulted in ozone changes less than 1%. These results confirm the above mentioned stable calibration level of the European regional standards in the past ten years.

The photograph of the Teide volcano proves why the Izaña Observatory on Tenerife is considered to be appropriate to perform Langley observations. If there are no clouds and no Sahara dust events normally the turbidity is extremely low, in addition the total ozone amount is rather constant. Only the TV antenna still makes some trouble with RFI on some Dobsons.

In addition to the calibration task another activity has become more and more important in the past years. Many of the operational instruments still had electronics of the seventies and therefore needed upgrading. A new electronics type, developed at the WDCC (NOAA, Boulder, USA) was slightly modified by MOHp and has been built into 25 Dobsons (23 at MOHp, 2 at Arosa by the Swiss colleagues) in the past years. Most of these Dobsons got a complete refurbishment of mechanics (new motors etc.) including optical refreshment with a new type of mirrors (better protective coating). Special highlight of

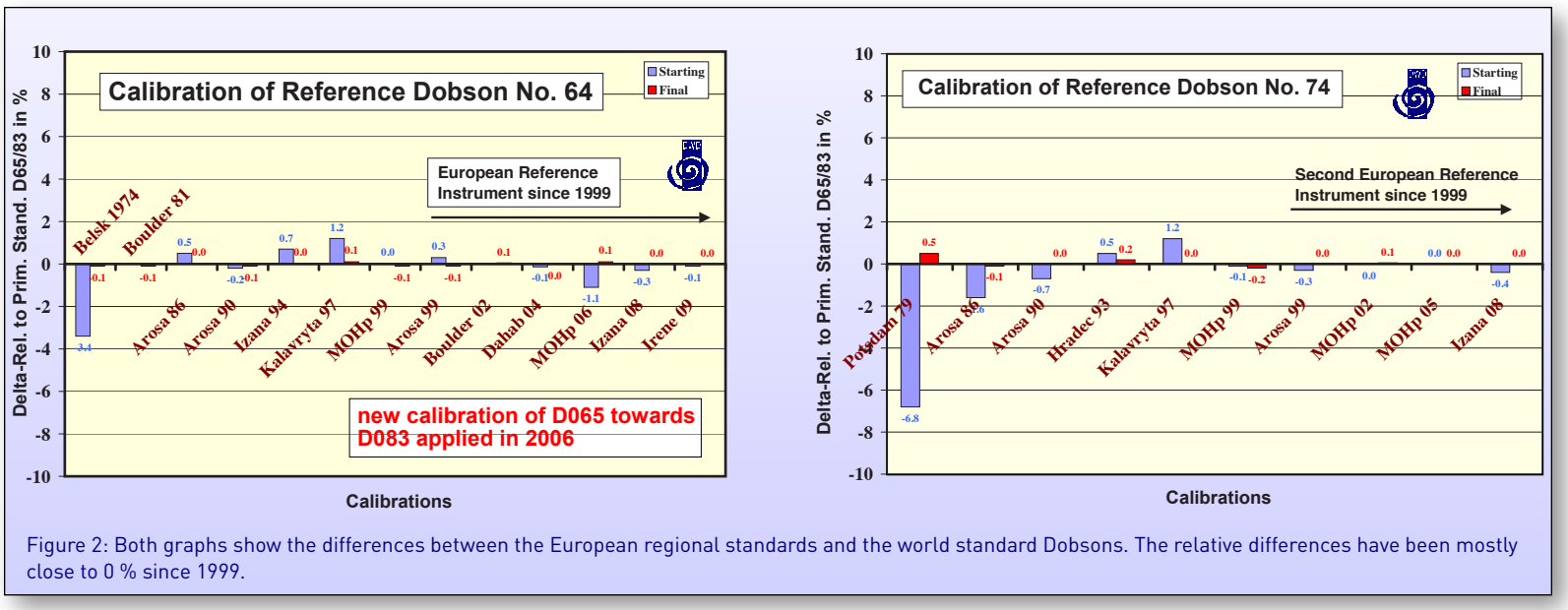

Figure 2: Both graphs show the differences between the European regional standards and the world standard Dobsons. The relative differences have been mostly close to 0 % since 1999.

Averages of Langley Corrections from the days 13, 16, 18, 20, 21, 22, 23, 24 Sep.2008

Instruments D064, D074 and D083 at Izana Observatory

With the existing Calibration, Lamp tests included

		Upper Mu limit	Lower Mu Limit	number in limits	Implied N correction	Std Deviation in N
D083	AD-Pairs			389.0	-0.2	0.4
		2.4	1.15	317.0	-0.2	0.5
		2.4	1.2	263.0	-0.1	0.4
D074	AD-Pairs			385.0	-0.6	0.7
		2.4	1.15	318.0	-0.5	0.8
		2.4	1.2	265.0	-0.6	0.6
D064	AD-Pairs			397.0	0.0	0.6
		2.4	1.15	327.0	0.3	0.6
		2.4	1.2	271.0	0.2	0.6

0.7N corresponds to 1.0 percent

Table 1: Averages of Langley Corrections for instruments D064, D074 and D083 during September 2008.

these activities were the upgrades of the four Dobsons of the British Antarctic Survey, which had been in use in Antarctica during the detection of the ozone hole and were still equipped with electronics of the fifties. The graph in Figure 3 evidently shows the success of the Dobson calibration system in the global ozone monitoring network during the past decades. The red diamonds, marked with red arrows, are these four BAS Dobsons, having not been regularly calibrated for many years: Only one instrument does not achieve the ±1 % difference for well calibrated instruments.

The following table gives an overview of all the activities in the past ten years. Electronic and optical refurbishment will come to a temporary end within the coming years, when the remaining European Dobsons will have been treated too. The focus will probably then be put on the relocation of Dobsons, which will no longer be used at European stations. This development will also facilitate the task of regular calibrations in the European network, as the number of operational Dobsons in Europe could significantly decrease. Another focus of the next decade will then be the support of establishing RDCC's like that in South Africa under the keyword "Capacity Building."

Although the first ten years of the RDCC-E at the Hohenpeissenberg have been full of work, sometimes with stress, when the Bavarian weather did not play along and the final calibration of instruments stood on a knife edge, but as summary it can be stated: Each Dobson left Hohenpeissenberg with a calibration and we met a lot of nice and interesting people

The Teide volcano, Spain's highest mountain, seen from the Izaña Observatory. Photo: Ulf Köhler.

from all around the world. The success and benefit of all these activities (of all Dobson calibration centres as well) for the data quality in the network is a good condition and qualification to continue this work for at least another ten years.

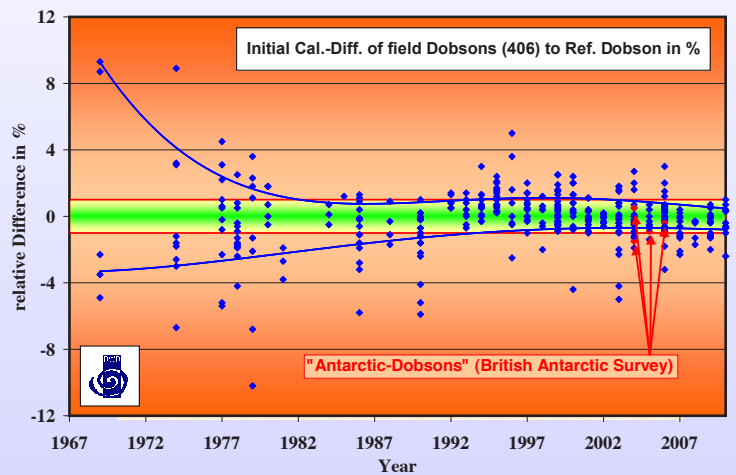

Figure 3: The blue diamonds show the relative difference of the calibrated Dobsons towards the used reference Dobsons during the initial calibration before any instrumental work was done. This difference represents the calibration status at the station.

Brewer User's Workshops

Brewer workshops took place in Aosta in September 2009 and in Beijing in September 2011. The report from the Aosta (and earlier workshops) can be found here: http://www.woudc.org/bdms/reports_e.html

The report from the Beijing workshop will be available at the same site.

Activities during ten years of RDCC-E operation	
Own campaigns at Mohp	18
Campaigns organized at other stations	8
Support for campaigns of other RDCC's	5
Sum	**31**
Calibrated Dobsons by RDCC-E	76
Calibration of Reference Dobsons	13
Support for Dobson calibrations of other RDCC's	25
Sum (from 27 countries)	**114**
Upgraded Dobsons	23
By Swiss colleagues	2
Sum	**25**
Relocated Dobsons	5

Table 2: RDCC-E activities during the last ten years.

News from the Infrared Working Group

The annual infrared working group meeting in May 2007 assembled more than 40 scientists.

Tropospheric δD profile measurements by ground-based FTIR

M. Schneider, F. Hase, T. Blumenstock, Institute for Meteorology and Climate Research - Atmospheric Trace Gases and Remote Sensing (IMK-ASF), Karlsruhe Institute of Technology (KIT), Leopoldshafen, Germany;
T. Warneke, Institute of Environmental Physics and Remote Sensing (IUP/IFE), University of Bremen, Germany

Water participates in many processes that are crucial for the Earth's climate. By distribution of heat (vertically and horizontally), regulating surface temperature, formation of clouds, radiative forcing due to water vapour, etc., it widely determines the energy budget and thus the climate of our planet. The isotopologue ratios of water (e.g. $HD^{16}O/H_2{}^{16}O$) are a powerful tool for investigating the different water cycle processes. In the following we express $H_2{}^{16}O$ and $HD^{16}O$ as H_2O and HDO, respectively, and $HD^{16}O/H_2{}^{16}O$ as
$\delta D = 1000‰ \bullet \{[[HD^{16}O]/[H_2{}^{16}O]] / SMOW\} - 1$, where $SMOW = 3.1152 \bullet 10^{-4}$ (SMOW: Standard Mean Ocean Water).

In the framework of NDACC ground-based FTIR experiments have been performed at about 25 globally distributed sites since many years and allow the generation of an unprecedented long-term data set of tropospheric δD with some global representativeness. Figure 1 shows column integrated δD retrieved from ship-borne FTIR measurements. These measurements reveal the "latitudinal effect", i.e., decreasing δD towards the poles.

Ground-based FTIR δD profiles

In Schneider et al. (2006) it is demonstrated that NDACC's high quality ground-based FTIR (Fourier Transform Infrared) spectrometer measurements can be used to retrieve δD profiles between the surface and the middle/upper troposphere.

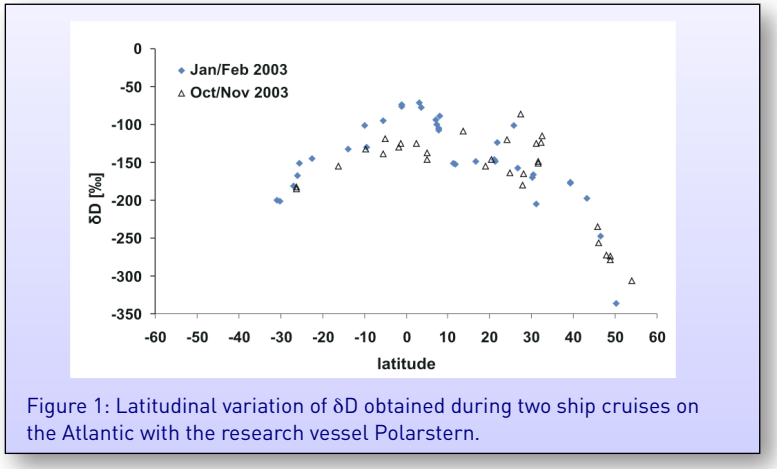

Figure 1: Latitudinal variation of δD obtained during two ship cruises on the Atlantic with the research vessel Polarstern.

The vertical resolution of these FTIR δD profiles is indicated by the averaging kernels shown in Fig. 2 for typical Kiruna and Izaña measurements. It is about 3 km in the lower troposphere and 6 km in the middle troposphere, with typical degrees of freedom of 1.6. Figure 2 also depicts the sum of all averaging kernels (thick solid black line), which indicates the total sensitivity of the FTIR system with respect to δD. For Kiruna the FTIR system is sensitive up to an altitude of 7 km (more than 75% of the atmospheric δD variability is detected by FTIR, see curve δ_{row}). For Izaña this sensitivity range is extended up to 10-11 km.

Theoretically, most errors cancel out by taking the ratio between HDO and H_2O. As leading δD error sources remain inconsistencies between the spectroscopic line parameters

of H_2O and HDO. For instance, an inconsistency of 1% between the pressure broadening parameters causes significant errors in the δD profile shape, whereby positive errors in the lower troposphere are correlated to negative errors in the middle/upper troposphere. For more details about the theoretical error estimation please refer to the extensive discussion in Schneider et al. (2006).

Figure 3 shows an example of time series of lower and middle tropospheric δD retrieved from Kiruna FTIR measurements of the 1996 to 2008 period.

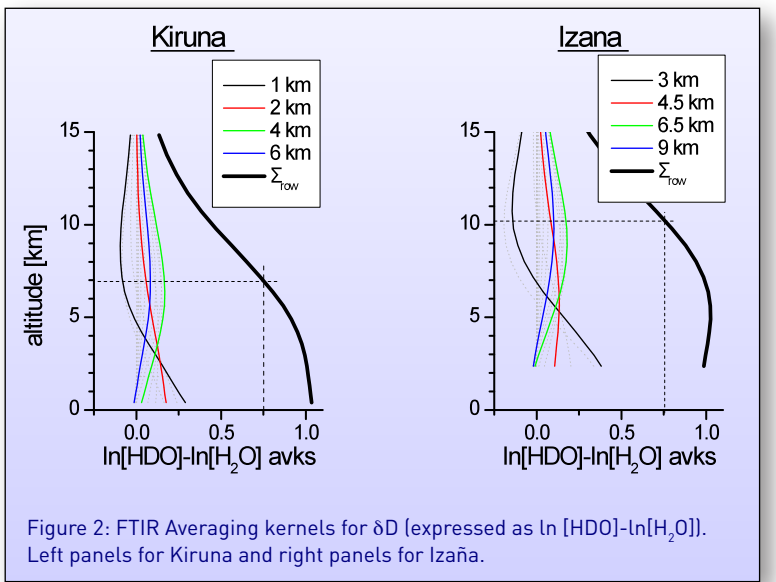

Figure 2: FTIR Averaging kernels for δD (expressed as ln [HDO]-ln[H_2O]). Left panels for Kiruna and right panels for Izaña.

Ground-based δD profile measurements for validating satellite data

Recently there has been large progress in observing tropospheric δD in vapour from space. The sensors TES (Tropospheric Emission Spectrometer, Worden et al., 2007) and SCIAMACHY (Scanning Imaging Absorption Spectrometer for Atmospheric Chartography, Frankenberg et al., 2009) have provided first global pictures of tropospheric δD, although for limited time periods of a few years only.

The vertical sensitivity of space-based tropospheric δD measurements is limited to the lower troposphere (for nadir sounders working in the near infrared, like SCIAMACHY) or to the middle troposphere (for nadir sounders working in the middle infrared, like TES). As a consequence the validation of the space-based observations requires δD profiles as a reference. The ground-based FTIR technique is the only technique that

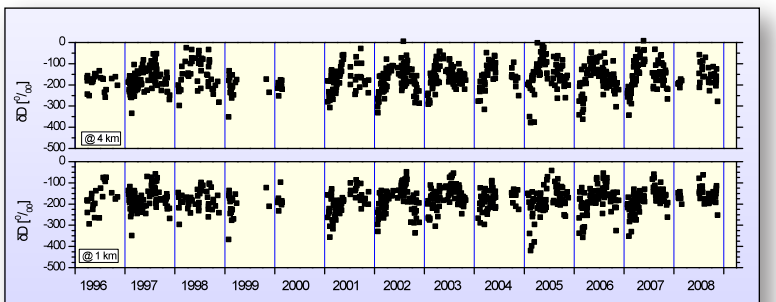

Figure 3. Time series of lower and middle tropospheric (altitude of 1 and 4 km, respectively) δD measured by the ground-based FTIR system at Kiruna.

can provide tropospheric δD profiles on a continuous basis. It is thus the only technique able to comprehensively validate the space-based measurements.

Long-term δD profile time series for constraining climate models

Long-term δD profile observations offer novel opportunities for investigating the atmospheric water cycle. An example is shown in Fig. 4, where the North Atlantic Oscillation index is plotted versus the middle tropospheric δD anomalies measured at the subtropical site of Izaña. The strong correlation indicates that the middle tropospheric water balance in the northern subtropics is significantly affected by pressure anomalies over the extra tropical northern Atlantic. The right panel shows the correlation for an atmospheric circulation model driven by prescribed sea surface temperature. The model does not well understand the subtropical water balance, which is of ultimate importance for climate on a global scale (the subtropics are the key region for the Earth's radiative cooling).

Without progress in modelling the water cycle, climate predictions will remain doubtful. The long-term δD time series produced from the ground-based FTIR measurements promise unprecedented opportunities for improving climate prediction models. For more details please refer to Schneider et al. (2010).

References

Frankenberg, C., K. Yoshimura, T. Warneke, I. Aben, A. Butz, N. Deutscher, D. Griffith, F. Hase, J. Notholt, M. Schneider, H. Schrejver, and T. Röckmann: Dynamic processes governing lower-tropospheric HDO/H_2O ratios as observed from space and ground, Science, 325, 1374–1377, 2009.

Hase, F., J.W. Hannigan, M.T. Coffey, A. Goldman, M. Höpfner, N.B. Jones, C.P. Rinsland, S.W. Wood (2004), Intercomparison of retrieval codes used for the analysis of high-resolution, ground-based FTIR measurements, *J. Quant. Spectrosc. Radiat. Transfer,* 87, 25-52.

Schneider, M., F. Hase, and T. Blumenstock: Ground-based remote sensing of HDO/H_2O ratio profiles: introduction and validation of an innovative retrieval approach, Atmos. Chem. Phys., 6, 4705-4722, 2006.

Schneider, M., F. Hase, T. Blumenstock (2006 a), Water vapour profiles by ground-based FTIR spectroscopy: study for an optimised retrieval and its validation, *Atmos. Chem. Phys*., 6, 811-830, SRef-ID: 1680-7324/acp/2006-6-811.

Schneider, M., K. Yoshimura, F. Hase, and T. Blumenstock: The ground-based FTIR network's potential for investigating the atmospheric water cycle, Atmos. Chem. Phys., 10, 3427-3442, 2010.

Worden, J. R., D. Noone, K. Bowman, R. Beer, A. Eldering, B. Fisher, M. Gunson, A. Goldman, R. Herman, S. S. Kulawik, M. Lampel, G. Osterman, C. Rinsland, C. Rodgers, S. Sander, M. Shephard, C. R. Webster, and H. Worden: Importance of rain evaporation and continental convection in the tropical water cycle, Nature, 445, 528--532, doi:10.1038/nature05508, 2007.

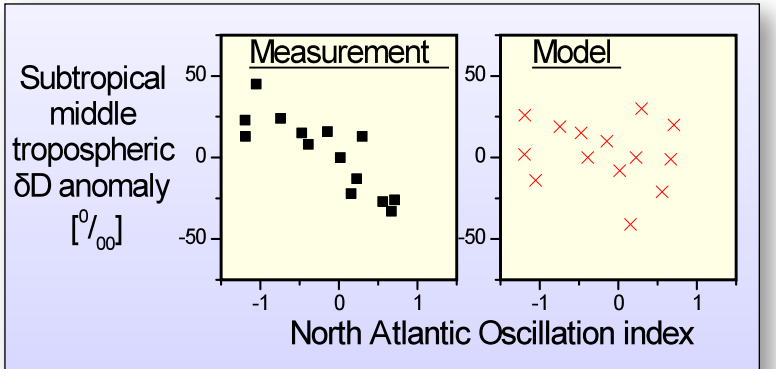

Figure 4: Correlation between the Northern Atlantic Oscillation index and subtropical middle tropospheric δD anomalies (shown are quarterly mean data). Left panel: FTIR measurements; Right panel: model simulations.

News from the UV-Visible Working Group

Stratospheric BrO measurement activities and archiving

Karin Kreher, National Institute of Water and Atmospheric Research (NIWA), Lauder, New Zealand and Michel van Roozendael, Belgian Institute for Space Aeronomy (BIRA-IASB), Brussels, Belgium

Despite its low abundance in the atmosphere, stratospheric bromine contributes up to 25% to the global ozone loss due to its high ozone depletion potential [e.g., World Meteorological Organization (WMO), 2007]. The main sources of bromine in the stratosphere are natural and anthropogenic long-lived and very short-lived brominated organic compounds [e.g., Pfeilsticker et al., 2000; Salawitch et al., 2005]. Long-term observations by in-situ ground-based networks have revealed a decline in total organic bromine from long-lived species by 3 to 5% during the 1998–2004 period [WMO, 2007].

In a recent study by Hendrick et al. [2008], the time evolution of stratospheric bromine monoxide (BrO) has been monitored since 1994 using UV-visible spectrometers operated at two stations of the NDACC: Harestua in Southern Norway (60°N, 11°E) and Lauder, New Zealand (45°S, 170°E). Results reveal a significant trend in stratospheric BrO evolving from positive values in the nineties to negative values in most recent years after 2000 (see Figure 1). Accounting for the mean age of air in the stratosphere, the decline in stratospheric bromine since 2002 is found to follow the reported decline of bromine long-lived source gases observed since the second half of 1998. These findings confirm that the impact of the Montreal Proto-

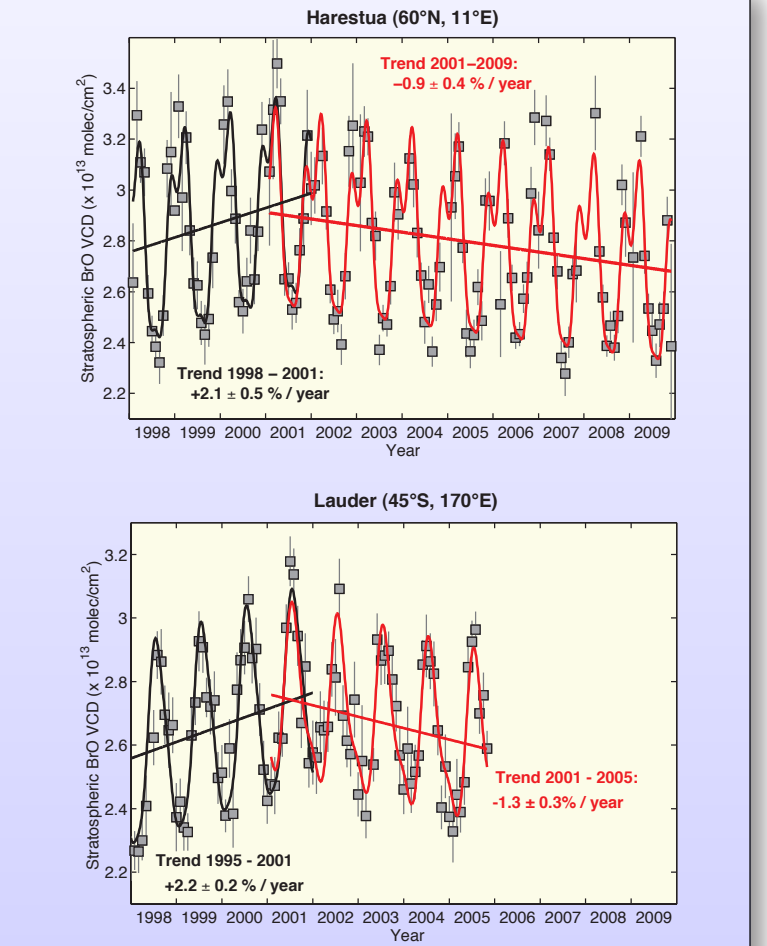

Figure 1: Trend analysis of stratospheric BrO columns over Harestua (60°N, 11°E; upper plot) and Lauder (45°S, 170°E; lower plot). More details in Hendrick et al. [2008].

col restrictions on brominated substances have now reached the stratosphere. Continued high quality NDACC observations of BrO columns and profiles will allow to monitor the future evolution of this important ozone related trace gas. These observations also constitute a key reference for the validation of BrO measurements from recent atmospheric chemistry satellite instruments, such as SCIAMACHY, GOME, GOME-2, OMI, MLS and JEM/SMILES [e.g. Hendrick et al., 2009].

Following a decision endorsed at the 2009 NDACC Steering Committee in Geneva, total column and stratospheric profile BrO measurements performed as part of the NDACC UV-Visible Working Group will be archived in the NDACC data base. In an effort to homogenize data sets and minimize risks of bias and inconsistencies in the retrieved quantities, BrO profiles derived using a commonly agreed Optimal Estimation inversion tool including treatment of the BrO diurnal photochemistry [Schofield et al., 2004; Hendrick et al., 2007] can be centrally produced at BIRA-IASB in agreement with measuring teams. Furthermore, intercomparisons of both BrO slant columns and vertical profile inversion methods are ongoing, e.g. as part of the recent CINDI campaign (see related Hot News on CINDI), and should lead to future consolidation of the NDACC BrO data products.

References

Hendrick, F., M. Van Roozendael, M. P. Chipperfield, M. Dorf, F. Goutail, X. Yang, C. Fayt, C. Hermans, K. Pfeilsticker, J.-P. Pommereau, J. A. Pyle, N. Theys, and M. De Mazière (2007), Retrieval of stratospheric and tropospheric BrO profiles and columns using ground-based zenith-sky DOASobservations at Harestua, 60°N, Atmos. Chem. Phys., 7, 4869–4885.

Hendrick, F., P.V. Johnston, K. Kreher, C. Hermans, M. De Mazière, and M. Van Roozendael (2008), One decade trend analysis of stratospheric BrO over Harestua (60°N) and Lauder (44°S) reveals a decline, Geophys. Res. Lett., 35, L14801, doi:10.1029/2008GL034154.

Hendrick, F., A. Rozanov, P. V. Johnston, H. Bovensmann, M. De Mazière, C. Fayt, C. Hermans, K. Kreher, W. Lotz, N. Theys, A. Thomas, J. P. Burrows, and M. Van Roozendael (2009), Multi-year comparison of stratospheric BrO vertical profiles retrieved from SCIAMACHY limb and ground-based UV-visible measurements, Atmos. Meas. Tech., 2, 273–285

Pfeilsticker, K., et al. (2000), Lower stratospheric organic and inorganic bromine budget for the artic winter 1998/99, Geophys. Res. Lett., 27, 3305– 3308.

Salawitch, R. J., D. K. Weisenstein, L. J. Kovalenko, C. E. Sioris, P. O. Wennberg, K. Chance, M. K. W. Ko, and C. McLinden (2005), Sensitivity of ozone to bromine in the lower stratosphere, Geophys. Res. Lett., 32, L05811, doi:10.1029/2004GL021504.

Schofield, R., Kreher, K., Connor, B. J., Johnston, P. V., Thomas, A., Shooter, D., Chipperfield, M. P., Rodgers, C. D., and Mount, G. H.(2004), Retrieved tropospheric and stratospheric BrO columns over Lauder, New Zealand, J. Geophys. Res., 109, D14304, doi:10.1029/2003JD004463.

World Meteorological Organization (WMO) (2007), Scientific assessment of ozone depletion: 2006, Global Ozone Res. Monit. Proj. Rep. 50, Geneva, Switzerland.

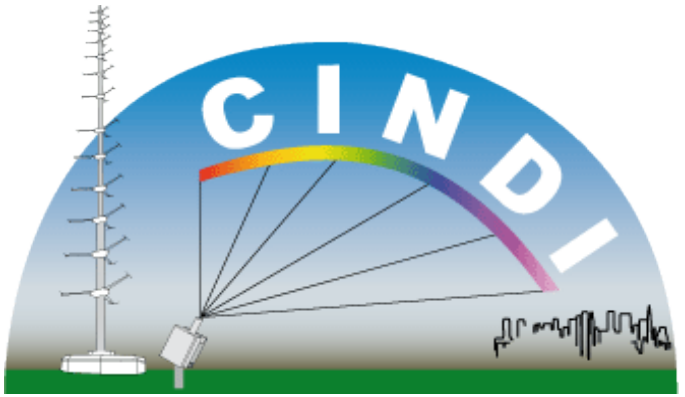

The CINDI campaign

Michel van Roozendael, Belgian Institute for Space Aeronomy (BIRA-IASB), Brussels, Belgium

In the period from June-July 2009, a large scale intercomparison of UV-Visible spectrometers took place at the Cabauw meteorological observatory, a semi-rural site located in the Netherlands, 30 km South of Utrecht. The main objective of this Cabauw Intercomparison Campaign of Nitrogen Dioxide measuring Instruments (CINDI) was to perform an extensive comparison of NO_2 measuring instruments that can be used in support of the validation of tropospheric NO_2 column measurements from satellites, with a strong emphasis on the assessment of tropospheric NO_2 column and profile measurements using the MAXDOAS technique. The campaign included a formal semi-blind exercise following standards from the Network for the Detection of Atmospheric Composition Change (NDACC), and was followed by a number of additional activities. In total measurements from 32 NO_2 instruments, most of them of DOAS type but also data from a NO_2 Lidar, in-situ sensors and a newly-developed NO2 sonde, were collected and intercompared. A number of additional parameters were also measured, including aerosol and other trace gases like HCHO, CHOCHO, BrO and ozone. Moreover special measurements were performed to study horizontal gradients in atmospheric composition and their impact on remote-sensing observations. After the campaign various working groups were set up to analyse results with the aim to progress towards improved and standardized retrieval algorithms. The campaign should result in consolidated trace gas and aerosol data products from both remote-sensing and in-situ techniques, thereby contributing to fulfil the needs for improved vertically-resolved monitoring of the air quality.

More information on the CINDI web-site:
http://www.knmi.nl/samenw/cindi/index.php

News from the Lidar Working Group

The Lidar Working Group during their meeting in June 2009 in Egbert, Ontario, Canada.

The Measurements of Humidity in the Atmosphere and Validation Experiments (MOHAVE) 2009 Campaign

Thierry Leblanc, NASA Jet Propulsion Laboratory, California Institute of Technology, Wrightwood, California, USA

The MOHAVE-2009 campaign took place on October 11-27, 2009 at the Jet Propulsion Laboratory (JPL) Table Mountain Facility in California (TMF, 34.4°N, 117.7°W). This third MOHAVE campaign involved more instruments and data sets than the two previous ones held in 2006 and 2007. The main objectives of the campaign were 1) to compare and validate the water vapour measurements (profile and total column) from several instruments including, two types of frost-point hygrometers, two types of radiosondes, four Raman lidars, two microwave radiometers, two Fourier-Transform spectrometers, and two GPS receivers; 2) to cover water vapour measurements from the ground to the mesopause without gaps; 3) to study upper tropospheric humidity variability at timescales varying from a few minutes to several days.

Nine of the participating instruments are currently affiliated to NDACC, namely, the TMF Raman lidar (T. Leblanc, JPL), the TMF tropospheric and stratospheric ozone differential absorption lidars (S. McDermid, JPL), and the microwave radiometer (G. Nedoluha, NRL), which are permanently deployed at Table Mountain, and the ALVICE mobile lidar (D. Whiteman, NASA/GSFC), AT and STROZ mobile lidars (T. McGee, NASA/GSFC), the mobile microwave radiometer MIAWARA-C (N. Kämpfer, Univ. of Bern), and the Fourier-Transform Infrared (FTIR) spectrometer MkIV (G. Toon, JPL), which were deployed at TMF for the duration of the campaign.

Because special focus was made on the water vapour lidars, the balloons were primarily launched during nighttime. A few launches were performed during daytime to accommodate the FTIR measurements, and Aura-TES Special Observations. Typically one frost-point hygrometer sonde, and three to four Vaisala RS92 radiosondes were launched each night, resulting in 20 frost-point sonde profiles and 58 radiosonde profiles over the 15-day-long campaign. The lidars operated as much as possible, with emphasis (full nights) during the three or four nights during New Moon (minimum sky background noise). The microwave measurements were quasi-continuous (day and night) throughout the campaign. Satellite coincidences comprised two close nighttime overpasses for Aura-MLS on October 11 and 27 (14 coincidences within 500 km), two Aura-TES daytime special observations on October 18 and 20, daily overpasses of Aqua-AIRS (within 200 km), four remote overpasses of ACE-FTS, and 18 ENVISAT-MIPAS coincidences within 500 km (three of them within 100 km).

A minor Pacific storm prevented most measurements on October 13-14. High clouds prevented lidar measurements in the first half of the night on October 21, and most of the night on October 27, and prevented FTIR measurements during the day on October 27. The rest of the campaign (i.e., more than ten nights) saw nearly cloud-free skies.

As mentioned above, two types of radiosondes were used during the campaign. Both types were systematically attached to the same balloon payloads. Non negligible differences in

the pressure (~0.5 hPa) and temperature (0.5-1 K) readings between the two radiosonde types were identified, and found to impact the derivation of water vapour mixing ratio and relative humidity by the Frost-Point hygrometers. The Cryogenic Frost-Point Hygrometer (CFH) and the National Oceanic and Atmospheric Administration Frost-Point Hygrometers (NOAA-FPH) showed excellent agreement in the stratosphere. The mean effect of the pressure reading differences between the two radiosonde types is shown for the CFH-derived mixing ratio in Fig. 1. In most cases (12 flights out of 16), these differences ran from +2% in the lower troposphere (wetter if using RS92 pressure) to -2% bias in the lower stratosphere (dryer if using RS92 pressure). Larger differences (up to ± 20%) of either sign (i.e., negative or positive) were observed on individual flights which, if studied on an altitude grid, result from a non-negligible shift in geopotential altitude.

Over 270 hours of water vapour nighttime measurements from three of the four Raman lidars were compared to that from the radiosondes and Frost-Point hygrometer sondes. The fourth lidar experienced failure and could not be operated until the very last day of the campaign. The JPL Raman lidar profiles reached 20 km when integrated all night, and 15 km when integrated for 1 hour. Because of the high variability of water vapour in the troposphere (standard deviation frequently exceeding 100% at timescales as short as two hours), two different approaches, depending on altitude range, were used for the comparisons involving the lidar measurements. For all altitudes below 13 km, only profiles obtained within 1 hour of each other were compared. Above 21 km, variability is reduced (standard deviations near 10%) and wider time windows (typically 4 hours) were chosen to increase the lidar precision. As

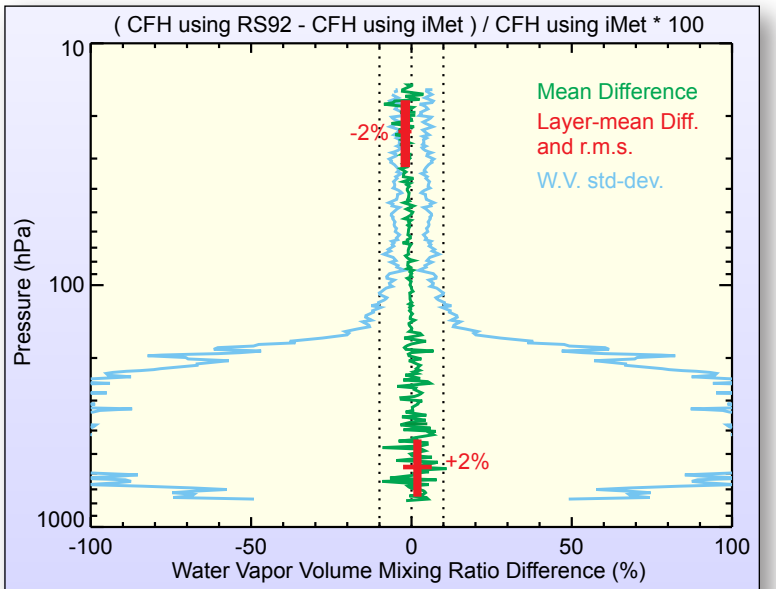

Figure 1: Effect of the differing pressure readings of the Vaisala RS-92 and Intermet PTU radiosondes on the derivation of water vapour mixing ratio by the Cryogenic Frost-Point Hygrometer; The 12 most stable balloon flights of MOHAVE-2009 were used.

shown in Fig. 2, excellent agreement between this lidar and the CFH was found throughout the measurement range, with only a 3% (0.2 ppmv) mean wet bias for the lidar with respect to CFH in the upper troposphere and lower stratosphere (UTLS). The two other operating water vapour lidars provided satisfactory results in the lower troposphere, but suffered from contamination by fluorescence, preventing their use in the UTLS (wet bias ranging from 5 to 50% between 10 km and 15 km).

In the stratosphere and mesosphere, the time coincidence criterion between WVMS (the radiometer from NRL), Aura-MLS, and MIAWARA-C (the radiometer from University of Bern) was widened up to 6 hours. A typical example of the measured profiles and their uncertainties is given in Fig. 3. Between 40 and 65 km, general agreement within 10% is found between all instruments. Below 40 km, MIAWARA-C was wetter than MLS, while throughout the stratosphere WVMS was generally drier than MLS. These discrepancies are currently under investigation.

Total Precipitable Water (TPW) measurements from six different co-located instruments were compared. For some of the instruments, several retrieval groups (JPL, NOAA, and the National Center for Atmospheric Research) provided their TPW solutions, resulting in the direct comparison of ten different datasets. Agreement within 10% (1 mm) was found between all datasets (Fig. 4). Such good agreement illustrates the maturity of these measurements, and significantly raised confidence levels for their use as an alternate and/or complementary source of calibration for the NDACC Raman lidars.

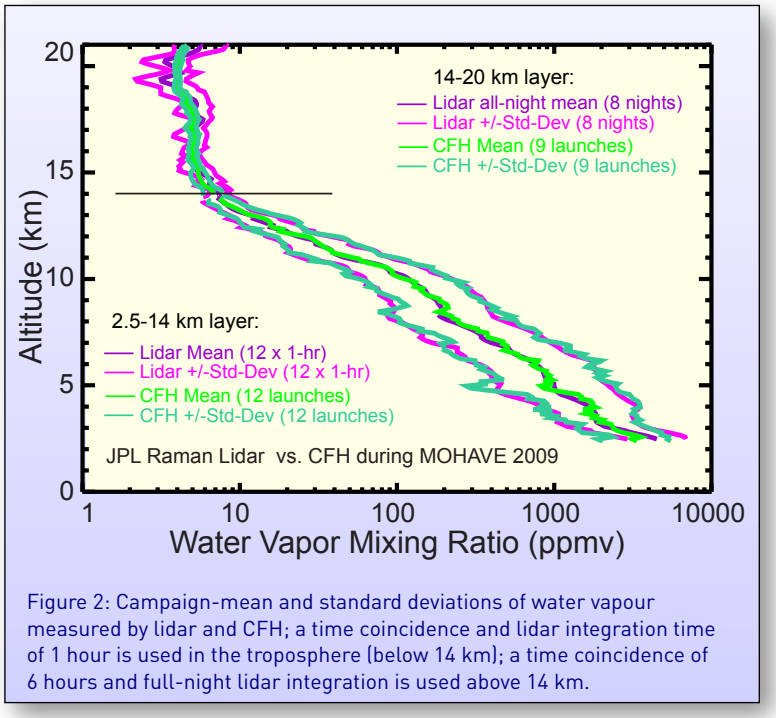

Figure 2: Campaign-mean and standard deviations of water vapour measured by lidar and CFH; a time coincidence and lidar integration time of 1 hour is used in the troposphere (below 14 km); a time coincidence of 6 hours and full-night lidar integration is used above 14 km.

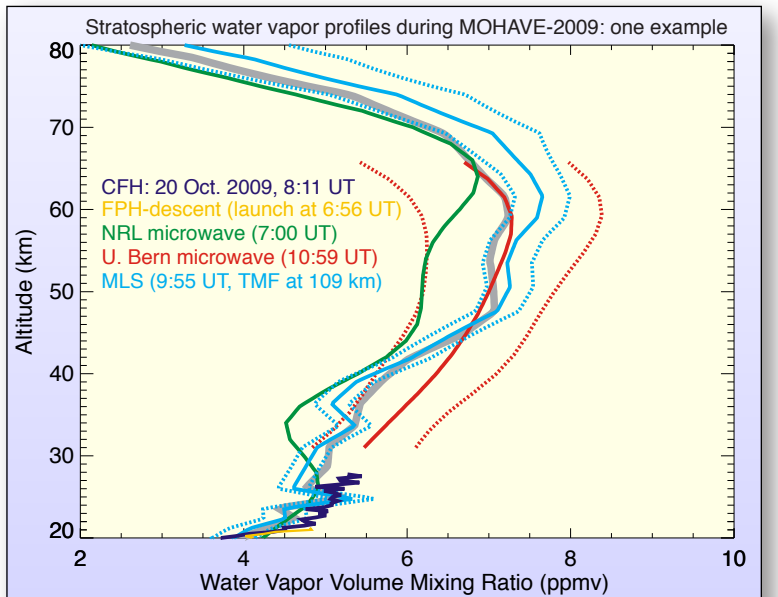

Figure 3: One example of simultaneous and co-located water vapour measurements, and their reported uncertainties, during MOHAVE-2009. The microwave measurements use 6-hour integration.

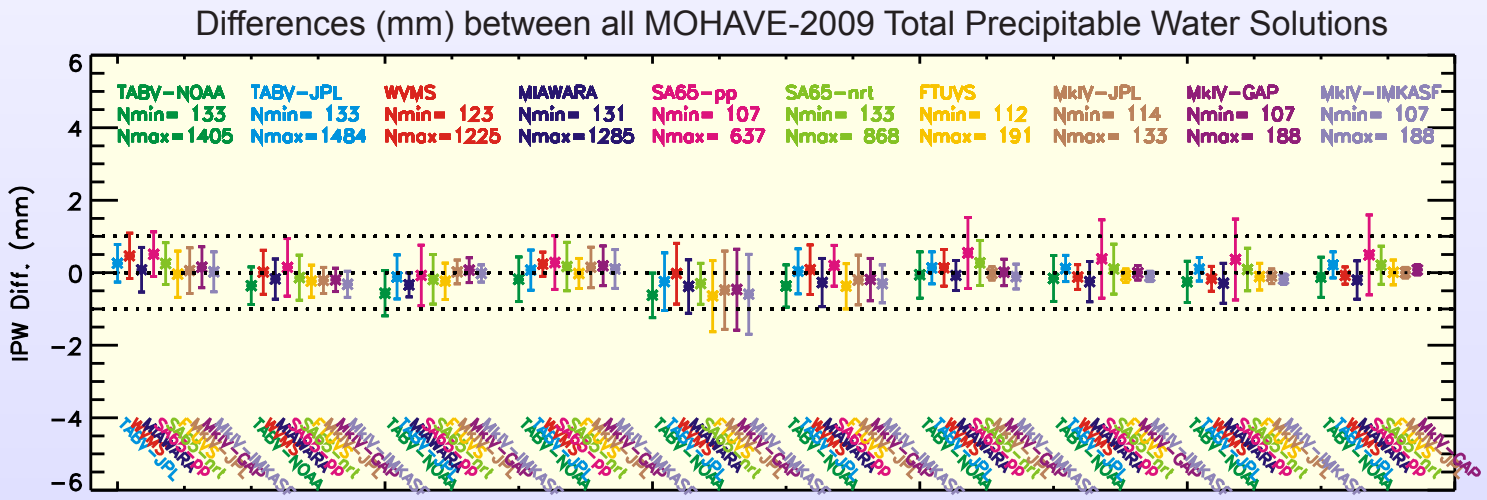

TABV-NOAA = TABV GPS receiver at TMF, solution by NOAA/GSD (Gutman/Holub)

TABV-JPL = TABV GPS receiver at TMF, solution by JPL (Haines)

WVMS = Microwave radiometer at TMF, solution by NRL (Nedoluha)

MIAWARA= MIAWARA-C microwave radiometer, solution by Univ. Bern (Straub/Kampfer)

SA-65 n.r.t. = SuomiNet GPS receiver, near-real-time solution by NCAR (Braun/Vanhove)

SA-65 p.p. = SuomiNet GPS receiver, alternate solution by NCAR (Braun/Vanhove)

FTUVS = Fourier-transform UV spectrometer at TMF, solution by JPL (Sander/Pongetti)

MkIV-JPL = Fourier-transform IR spectrometer MkIV, solution by JPL (Toon/Blavier)

MkIV-GAP = Fourier-transform IR spectrometer MkIV, solution by IMK/IFU (Sussmann)

MkIV-IMKASF = Fourier-transform IR spectrometer MkIV, solution by IMK-ASF (Schneider)

Figure 4: Comparison between all Total Precipitable Water Measurements made during MOHAVE-2009 (6 instruments, multiple retrievals for some instruments); Nmin and Nmax refer to the minimum and maximum number of pairs used for the comparisons; the vertical bars show the r.m.s. of the differences.

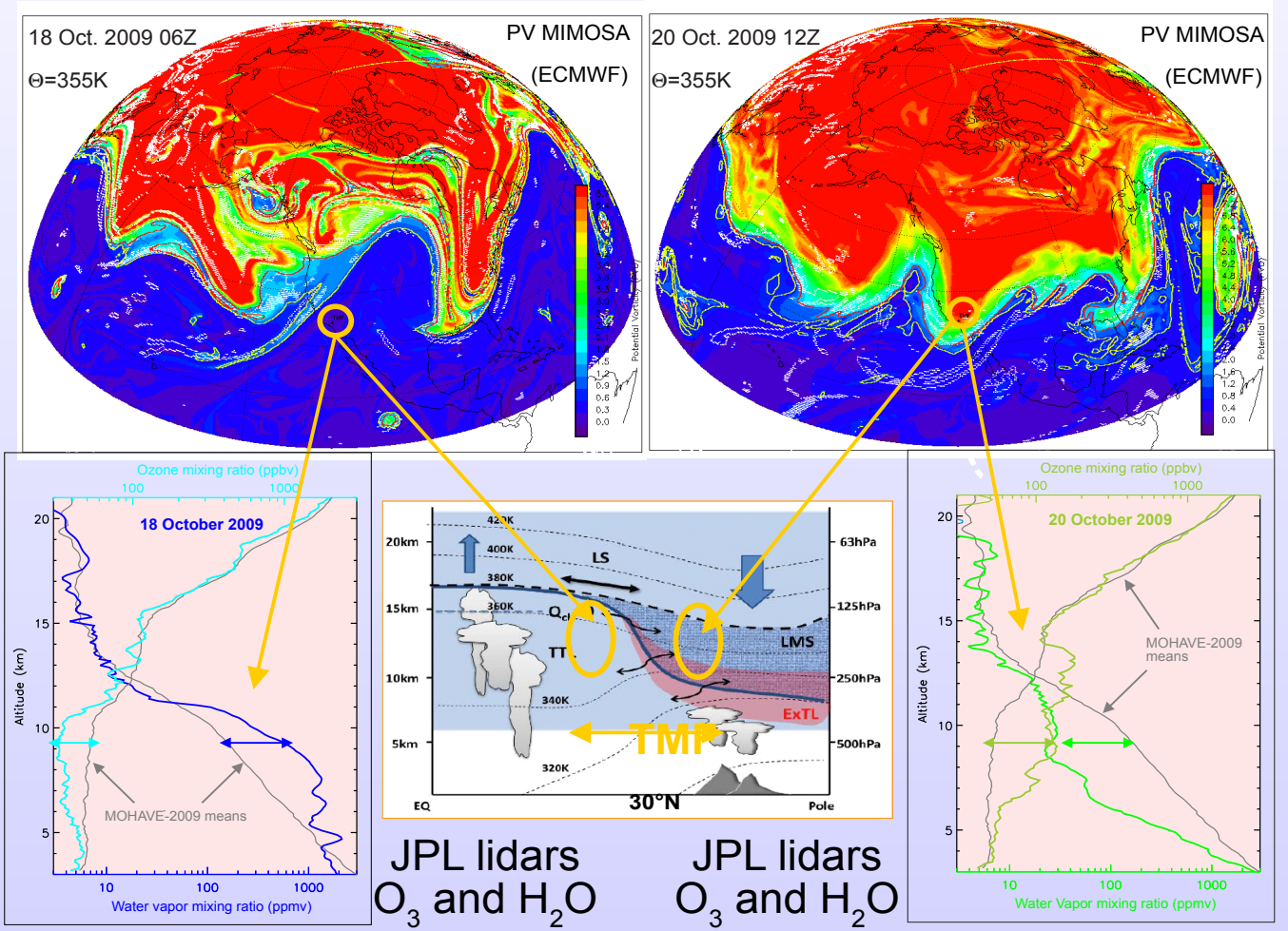

Figure 5: Schematic view, and demonstration by the observations, of what the JPL/TMF water vapour and ozone lidars sample when sounding layers located either north or south of the subtropical jet; top figures: Potential Vorticity maps produced by the high-resolution model MIMOSA.

Tropospheric and stratospheric ozone and temperature measurements were also obtained from differential absorption lidar and ECC ozonesondes. The water vapour and ozone measurements, together with the advected potential vorticity results from the high-resolution transport model MIMOSA and back-trajectory calculations, allowed the identification of a stratospheric intrusion over TMF on October 20. Ozone-water vapour anti-correlation typically holds, with the alternation of ozone-rich and dry air masses originating in the lowermost extra-tropical stratosphere, and ozone-poor and humid air masses originating in the subtropical upper troposphere. An example of the contrasting air masses sampled by lidar is shown on Fig. 5 (Oct. 18 vs. Oct. 20). Isentropic backward trajectories computed for selected altitudes and dates confirmed this relationship, as illustrated by Fig. 6 (colour-coded by ozone and water vapour anomalies). Interestingly, the typical anti-correlation relation broke down shortly after the stratospheric intrusion event of Oct. 20, where significant mixing seemed to have taken place along the subtropical jet during the few days preceding the TMF event (not shown).

The numerous results from MOHAVE-2009 have shown the critical importance of such multi-techniques comparison campaigns. On one hand, they remind us that the measurements of water vapour in the UTLS remains a contemporary challenge. On the other hand, they provide new confidence in the future simultaneous detection by lidar of long-term variability of water vapour and ozone in the UTLS.

The MOHAVE-2009 Team

T. Leblanc, T. D. Walsh and I. S. McDermid, Jet Propulsion Laboratory, California Institute of Technology, Wrightwood, CA (water vapour Raman Lidar, tropospheric DIAL, stratospheric DIAL, Vaisala RS92 PTU radiosondes, Intermet PTU radiosondes)

D. Hurst, E. Hall, A. Jordan, NOAA Global Monitoring Division, Boulder, CO (NOAA-Frost Point Hygrometer)

H. Vömel, German Weather Services (DWD), Lindenberg, Germany (Cryogenic Frost Point Hygrometer)

D. W. Whiteman, H. Selkirk, NASA Goddard Space Flight Center, Greenbelt, MD, D. Venable, A. Dirisu, Howard Univ., Beltsville, MD (ALVICE mobile lidar, Vaisala RS92 PTU radiosonde, GPS-Suominet SA65)

T. G. McGee, L. Twigg, G. Sumnicht, NASA Goddard Space Flight Center, Greenbelt, MD (STROZ-light mobile lidar, AT mobile lidar)

G. Toon, J.-F. Blavier, Jet Propulsion Laboratory, California Institute of Technology, Pasadena, CA (Fourier-Transform Infrared Spectrometer MkIV)

L. Miloshevich, Milo Inc., Boulder, CO (groundbased PTU, Vaisala RS92 PTU radiosondes)

C. Straub, N. Kampfer, Univ. Of Bern, Switzerland (MIAWARA-C microwave radiometer)

G. Nedoluha, M. Gomez, Navy Research laboratory, Washington, D.C. (WVMS microwave radiometer)

S. Sander, T. Pongetti, Jet Propulsion Laboratory, California Institute of Technology, Pasadena, CA (Fourier-Transform UV Spectrometer)

A. Hauchecorne, LATMOS, France (MIMOSA-PV real-time forecast)

G. Stiller, Univ. Karlsruhe, Germany (ENVISAT-MIPAS)

K. Walker, Univ. Toronto, Canada (ACE-FTS, MAESTRO)

B. Haines (JPL), S. Gutman (NOAA) , K. Holub (NOAA), J. Braun (NCAR), T. Vanhove (NCAR), GPS column water retrievals.

B. Read (Aura-MLS), B. Herman, (Aura-TES), E. Fetzer and E. Manning (Aqua-AIRS)

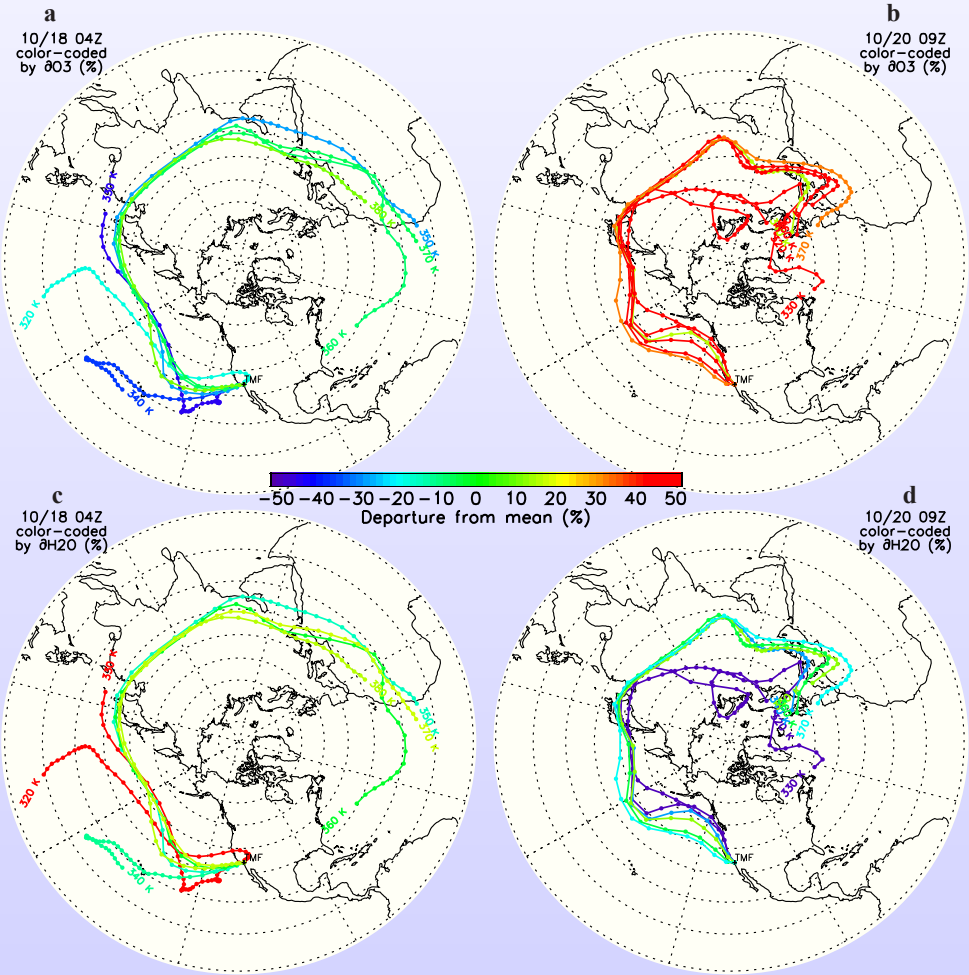

Figure 6: Selected 10-day back-trajectories ending over TMF on Oct. 18 (left) and 20 (right), 2009; top row: trajectories are colour coded by ozone anomalies with respect to the MOHAVE-2009 campaign mean; bottom row: trajectories are colour coded by water vapour anomalies.

News from the Microwave Working Group

Zimmerwald observatory located at 46.88°N, 7.47°E and 905.5 masl. Photo: Geir Braathen

Extending the Altitude Range of Ground-Based Microwave Water Vapour Measurements

Gerald Nedoluha, United States Naval Research Laboratory, Washington DC, USA

The Water Vapour Mm-wave Spectrometer (WVMS) instruments have been providing measurements of water vapour from NDACC sites since the early 1990s [Nedoluha et al., 1995; Nedoluha et al., 2009]. The upper limit measurement altitude of the technique is governed by the altitude at which the spectral line is predominantly Doppler, rather than pressure broadened, which occurs at approximately 80 km for this water vapour transition, above which there is no longer a strong dependence of the line shape on altitude. However, the lower limit altitude for retrievals is governed by instrumental considerations and not the physics of the measurement. Based on the success of this technique for monitoring mesospheric and upper stratospheric water vapour, there has been a large impetus in the community to increase the measurement spectral bandwidth and, thereby, extend the measurements down into the lower stratosphere [e.g. Deuber et al., 2005]. There are two major difficulties associated with this extension: instrumental spectral baseline issues, and the large variability of the tropospheric water vapour profile.

Keeping an instrumental spectral baseline stable over an extended period of time is extremely difficult. In Figure 1 [Nedoluha et al., submitted] we show that it was possible to provide measurements which are agreed well with measure-

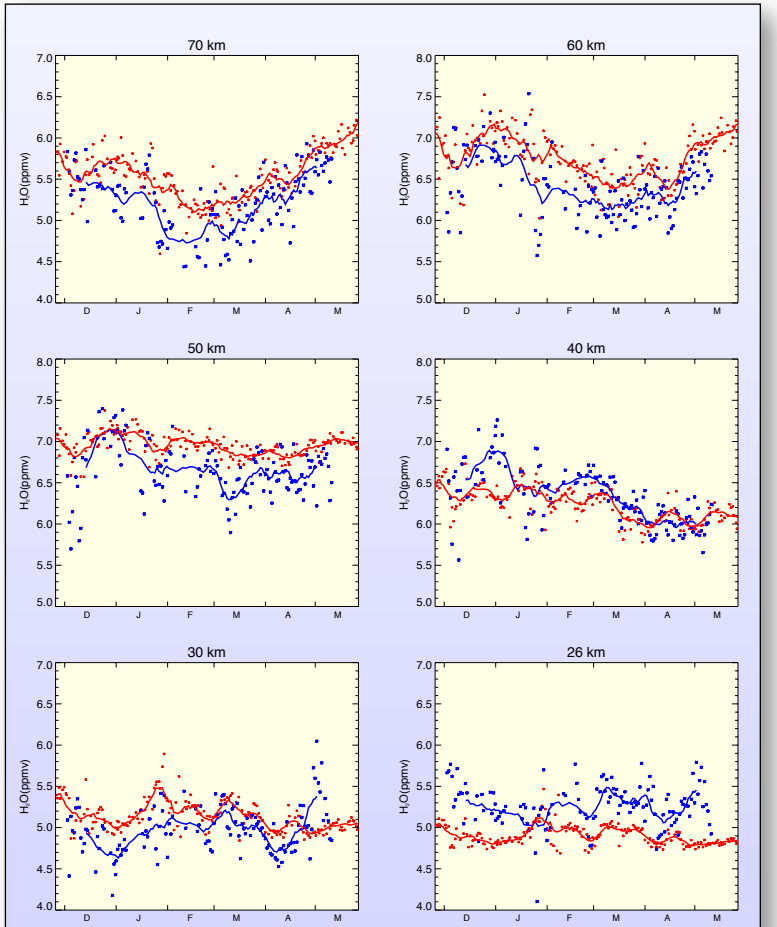

Figure 1: WVMS (blue) and convolved MLS (red) daily retrievals in the middle atmosphere over Table Mountain from December 2008 to May 2009. The lines show a 10-point smoothing.

ments from AURA MLS down to ~26 km over a 5+ month period at Table Mountain, California. The measurements at 26 km show little change during this period, but we note that the instrument is sensitive at this altitude, and therefore would show larger variations in water vapour if these did occur. Work is currently underway to extend this capability to WVMS observations from Mauna Loa, Hawaii.

The large amount of water vapour in the troposphere creates an additional problem for measurements of water vapour in the stratosphere, since it can be difficult for retrievals to distinguish emission in the upper troposphere from that in the lower stratosphere. For Table Mountain, a very dry high altitude site, this uncertainty has been characterized and introduces an error at ~26 km of ~4%. For sites with higher tropospheric humidity this error will be larger.

Although measurements in the mesosphere are sufficient for the detection of long-term trends, they do not always capture the shorter-term multi-year variations such as the increase in stratospheric water vapour which was observed by in 2001 [Randel, 2006]. The establishment of a stable set of measurements down to ~26 km will therefore provide an important extension to the ability of ground-based microwave systems to measure changes in water vapour entering the stratosphere.

References

Deuber, B., et al. (2005), Middle Atmospheric Water Vapour Radiometer (MIAWARA): Validation and first results of the LAPBIAT Upper Tropospheric Lower Stratospheric Water Vapour Validation Project (LAUTLOS-WAVVAP) campaign, J. Geophys. Res., 110, D13306, doi:10.1029/2004JD005543.

Nedoluha, G. E., et al. (1995), Ground-based measurements of water vapour in the middle atmosphere, J. Geophys. Res., 100, 2927-2939, 1995.

Nedoluha, G. E., et al (2009), Water vapour measurements in the mesosphere from Mauna Loa over solar cycle 23, J. Geophys. Res., 114, D23303, doi:10.1029/2009JD012504, 2009

Nedoluha, G. E., et al. (2011), Ground-based Microwave Measurements of Water Vapor from the mid-Stratosphere to the Mesosphere, J. Geophys. Res., 116, doi:10.1029/2010JD014728, 2011.

Randel, W. J., et al. (2006), Decreases in stratospheric water vapour after 2001: Links to changes in the tropical tropopause and the Brewer-Dobson circulation, J. Geophys. Res., 111, D12312, doi:10.1029/2005JD006744, 2006.

The WVMS instrument at Table Mountain. Photo: Gerald Nedoluha.

News from the Theory and Analysis Working Group

Evaluating Chemistry-Climate Models Using NDACC Data

Martyn Chipperfield, University of Leeds, UK and Bill Randel, National Center for Atmospheric Research (NCAR), Boulder, Colorado, USA

Coupled three-dimensional chemistry-climate models (CCMs) are our main tool for predicting the future evolution of atmospheric composition. These models are very complex and computationally expensive. Assessing their performance is a challenging task but essential if we are to have confidence in their predictions. Recently, the atmospheric modeling community has undertaken an extensive evaluation of 18 stratospheric CCMs from groups worldwide. This CCMVal project, organised within SPARC (Stratospheric Processes and Their Role in Climate), involved over 100 scientists who analysed the radiative, dynamical, transport and chemical processes in the models in unprecedented detail. The report has recently been published (SPARC CCMVal, 2010).

NDACC observations were used in the evaluation of the CCMVal models. In particular, the long time series of NDACC observations were crucial for evaluating the past trends produced by the models. Figure 1 (next page), taken from the CCMVal report, compares the observed columns of the main stratospheric chlorine reservoirs at the Jungfraujoch station with 14 models. The observations show an increase in chlorine (i.e. HCl + $ClONO_2$) until about 2000 followed by a decrease. This reflects the success of the Montreal Protocol in reducing the emission of chlorine-containing source gases. The CCMs are forced by the surface boundary condition of the observed chlorine source gases. The models then calculate the decomposition of these source gases into reservoirs such as HCl and $ClONO_2$. While all models simulate the increase and levelling off in chlorine, there are significant differences in the accuracy of models. Some models greatly over or underestimate the observed chlorine columns. This illustrates that more work is needed by the modeling community to improve the performance of the models and thereby reduce the uncertainty of future atmospheric changes in response to reduced chlorine source gas emissions.

Reference

SPARC CCMVal (2010), SPARC Report on the Evaluation of Chemistry-Climate Models, V. Eyring, T.G. Shepherd, D.W. Waugh (Eds.), SPARC Report No. 5, WCRP-132, WMO-TD-No 1526.

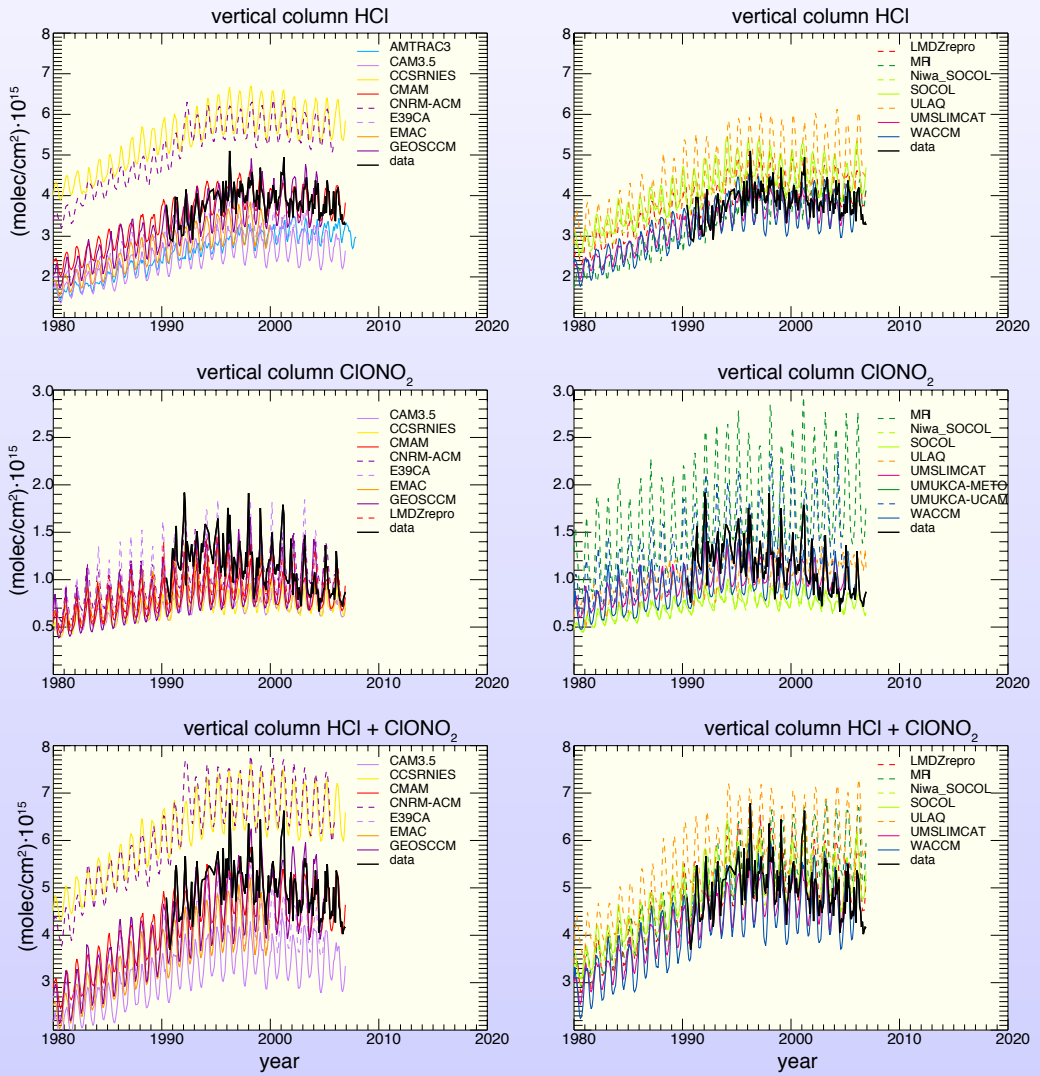

Figure 1. Comparison of NDACC observed column abundances (molecules·cm^{-2}) of HCl, $ClONO_2$, and their sum at Jungfraujoch (45°N) with output from 14 different CCMs from different groups. The models are divided arbitrarily between the left and right hand columns. Taken from SPARC CCMVal (2010) Chapter 6.

Report from the NDACC Data Host Facility

Jeannette Wild and Roger Lin, National Oceanic and Atmospheric Administration National Center for Environmental Prediction (NOAA/NCEP), Camp Springs, Maryland, USA

Data transfers returned to approximately 70,000 files per month (Figure 1) after being out of service for a time in 2006. From late 2008 until late 2010 the monthly count was around 90,000 files. The last year, from October 2010 to September 2011, the monthly file count has been a bit above 60,000 files on average. You can find the NDACC public data set and its description via its web site at http://www.ndacc.org/, or directly via anonymous ftp at ftp://ftp.cpc.ncep.noaa.gov/ndacc.

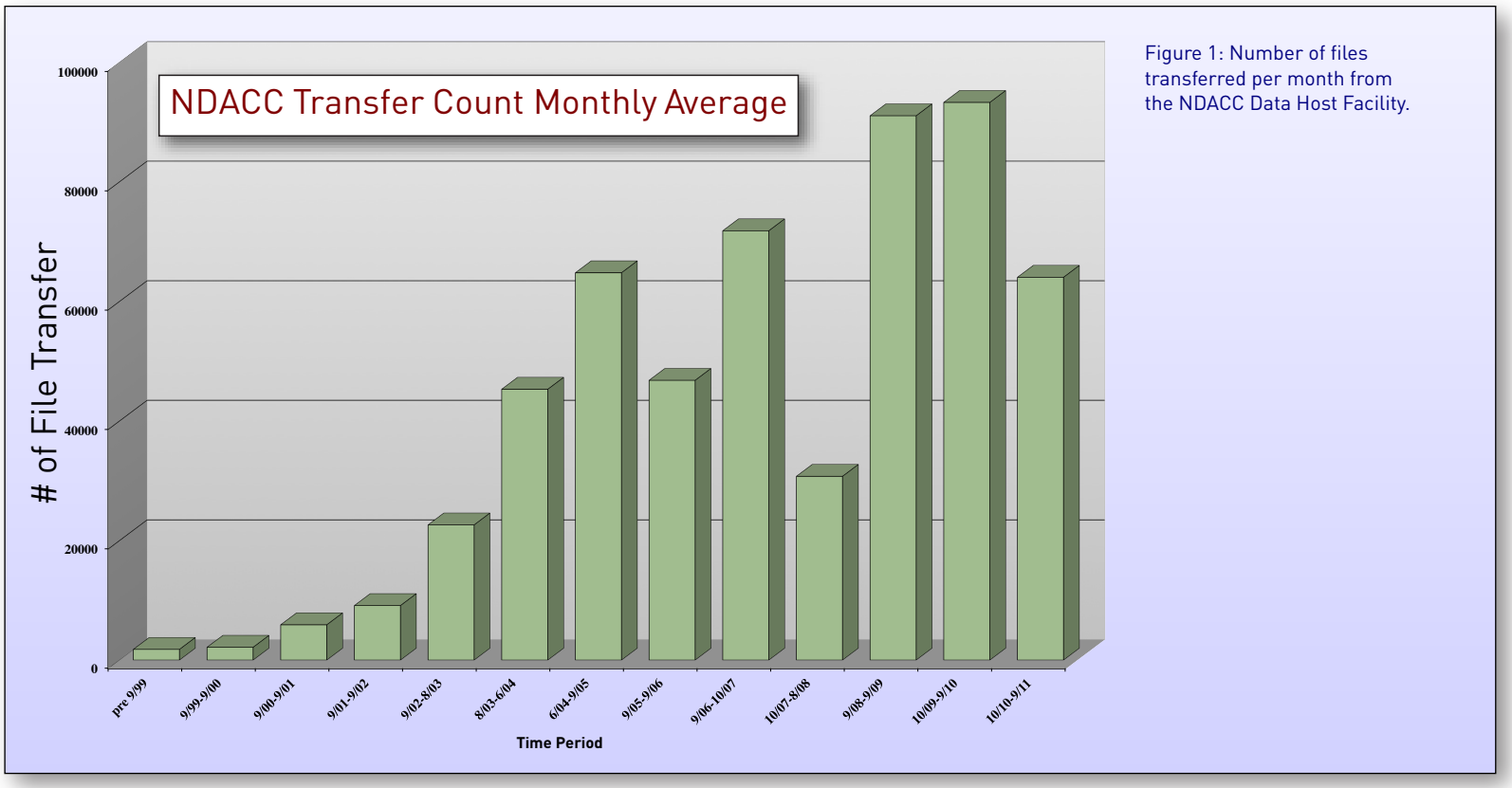

Figure 1: Number of files transferred per month from the NDACC Data Host Facility.

Meetings

The 2008 Steering Committee meeting

The 2008 meeting of the NDACC Steering Committee took place in Kangerluusuaq and Illulissat, Greenland from 25-30 September.

The 2009 Steering Committee meeting

The 2009 meeting of he NDACC Steering Committee took place in Geneva, Switzerland from 29 Sept to 1 October. On 2nd of October there was a visit to the NDACC station at Payerne.

The 2010 Steering Committee meeting

The 2010 meeting of he NDACC Steering Committee took place in Queenstown, New Zealand from 5 to 7 October with a visit to the Lauder station on 8 October.

Participants at the 19th NDACC Steering Committee meeting in Greenland in September 2008. Photo: Geir Braathen.

Participants at the 20th NDACC Steering Committee meeting in Geneva in September/October 2009. Photo: Chantal Renaudot and Geir Braathen.

Participants at the 21st NDACC Steering Committee meeting in Queenstown in October 2010. Photo: Geir Braathen.

The international Network for the Detection of Atmospheric Composition Change (NDACC) was formed to provide a consistent, standardised set of long-term measurements of atmospheric trace gases, particles, and physical parameters via a suite of globally distributed sites.

The principal goals of the network are:

- To study the temporal and spatial variability of atmospheric composition and structure in order to provide early detection and subsequent long-term monitoring of changes in the physical and chemical state of the stratosphere and upper troposphere; in particular to provide the means to discern and understand the causes of such changes.
- To establish the links between changes in stratospheric ozone, UV radiation at the ground, tropospheric chemistry, and climate.
- To provide independent calibration and validation of space-based sensors of the atmosphere and to make complementary measurements.
- To support field campaigns focusing on specific processes occurring at various latitudes and seasons.
- To produce verified data sets for testing and improving multidimensional models of both the stratosphere and the troposphere.

The primary instruments and measurements of NDACC are:

- Ozone lidar (vertical profiles of ozone from the tropopause to at least 40 km altitude; in some cases tropospheric ozone will also be measured)
- Temperature lidar (vertical profiles of temperature from about 30 to 80 km)
- Aerosol lidar (vertical profiles of aerosol optical depth in the lower stratosphere)
- Water vapour lidar (vertical profiles of water vapour in the lower stratosphere)
- Ozone microwave (vertical profiles of stratospheric ozone from 20 to 70 km)
- H_2O microwave (vertical profiles water vapour from about 20 to 80 km)
- ClO microwave (vertical profiles of ClO from about 25 to 45 km, depending on latitude)
- Ultraviolet/Visible spectrograph (column abundance of ozone, NO, and, at some latitudes, OClO and BrO)
- Fourier Transform Infrared spectrometer (column abundances of a broad range of species including ozone, HCl, NO, NO_2, $ClONO_2$, and HNO_3)
- Ozone and aerosol sondes (vertical profiles of ozone concentration and aerosol backscatter ratio)
- UV spectroradiometers (absolutely calibrated measurements of UV radiance and irradiance)

Contacts

For more information, please go to the NDACC web site (http://www.ndacc.org) or contact the co-chairs:

Dr. Michael J. Kurylo
Goddard Earth Sciences and Technology (GESTAR) Program
Universities Space Research Association
NASA Goddard Space Flight Center
Mail Stop 610.6
8800 Greenbelt Road
Greenbelt, MD 20771, USA
E-mail: Michael.J.Kurylo@nasa.gov

Dr. Geir O. Braathen
Atmospheric Environment Research Division (AER)
Research Department (RES)
World Meteorological Organization (WMO)
Case postale 2300
CH-1211 Geneva 2, Switzerland
E-mail: GBraathen@wmo.int

NDACC